Soft Matter

PAPER

View Article Online
View Journal | View Issue

Cite this: *Soft Matter*, 2016, 12, 4007

Received 12th February 2016,
Accepted 8th March 2016

DOI: 10.1039/c6sm00367b

www.rsc.org/softmatter

Active colloids at fluid interfaces

P. Malgaretti,*[ab] M. N. Popescu[ab] and S. Dietrich[ab]

If an active Janus particle is trapped at the interface between a liquid and a fluid, its self-propelled motion along the interface is affected by a net torque on the particle due to the viscosity contrast between the two adjacent fluid phases. For a simple model of an active, spherical Janus colloid we analyze the conditions under which translation occurs along the interface and we provide estimates of the corresponding persistence length. We show that under certain conditions the persistence length of such a particle is significantly larger than the corresponding one in the bulk liquid, which is in line with the trends observed in recent experimental studies.

1 Introduction

Micro- and nanometer scale particles capable of self-inducing motility within liquid environments[1–5] are promising candidates for the development of novel lab-on-a-chip cell-sorting devices, chemical sensors,[6] or targeted-drug-delivery systems,[7] to cite just a few potential applications. One proposal, which has generated significant experimental and theoretical attention within the last decade (see, *e.g.*, the recent reviews in ref. 1, 3 and 4), is to achieve self-motility by designing "active" particles capable of inducing chemical reactions within the surrounding liquid. One such system, which will be of particular interest for the present study, is represented by spherical beads partially covered over a spherical cap region by a catalyst which promotes, in the suspending solution, a chemical conversion of reactants ("fuel") into product molecules.† Due to the partial coverage by the catalyst, the spherical symmetry of the system is broken in two ways. First, the material properties of the particle vary across the surface and an axis of symmetry, which passes through the center of the particle and the pole inside the catalyst covered cap, can be defined. Second, the chemical reaction takes place only on the catalytic part of the surface, and therefore the chemical composition of the surrounding solution is varying along the surface of the particle. The out-of-equilibrium chemical composition gradients along the surface, due to the chemical reaction, couple to the particle *via* the interactions of the molecules in solution with the surface of the particle. This interplay eventually leads to hydrodynamic flows and to the motion of the particle relative to the solution, analogous to classic phoresis.[8,9] The active motion of such particles in the homogeneous bulk of the fluids has been the subject of numerous experimental (see, *e.g.*, ref. 1, 3, 4, 10 and 11) and theoretical (see, *e.g.*, ref. 9 and 12–15) studies.

However, in many cases such active Janus particles are suspended in a solution bound by a liquid–fluid interface, which raises several new issues. It is known that in thermal equilibrium, *i.e.*, in the absence of such motility-promoting chemical reactions, owing to their amphiphilic nature Janus particles tend to accumulate at liquid–fluid interfaces. (This effect can be exploited, *e.g.*, for the stabilization of binary emulsions.[16–18]) If the Janus particles are trapped at and confined to liquid–fluid interfaces their collective behavior, *e.g.*, when externally driven or when relaxing towards equilibrium after a perturbation, can be strongly affected by this quasi two-dimensional (2D) confinement itself and by interface-promoted interactions, such as capillary interactions (see, *e.g.*, ref. 19–21).

For an active Janus colloid, being trapped at the interface (*i.e.*, being unable to move in the direction normal to the interface; see, *e.g.*, ref. 22 for recent experimental results) can, on the one hand, affect the particle dynamics due to the effects discussed above. On the other hand, this trapping may induce novel self-propulsion mechanisms. For example, it has been recently predicted that if one of the reaction products exhibits a preference for the surface and thus tends to accumulate at the interface, the trapped Janus sphere will be set into motion along the interface by Marangoni flow, induced by the spatially non-uniform distribution of the reaction products.[23,24] (A similar motility mechanism can originate from thermally induced Marangoni flows, *e.g.*, if the Janus particle contains a metal cap which is heated by a laser beam;[25] furthermore, as reported

[a] *Max-Planck-Institut fur Intelligente Systeme, Theory of Inhomogeneous Condensed Matter, Heisenbergstrasse 3, Stuttgart, Germany. E-mail: malgaretti@is.mpg.de*
[b] *IV Institut für Theoretische Physik, Universität Stuttgart, Pfaffenwaldring 57, D-70569 Stuttgart, Germany*

† Such particles, which have distinct material properties across the two regions of their surface, are often called Janus particles; in the following we shall use this notation, too.

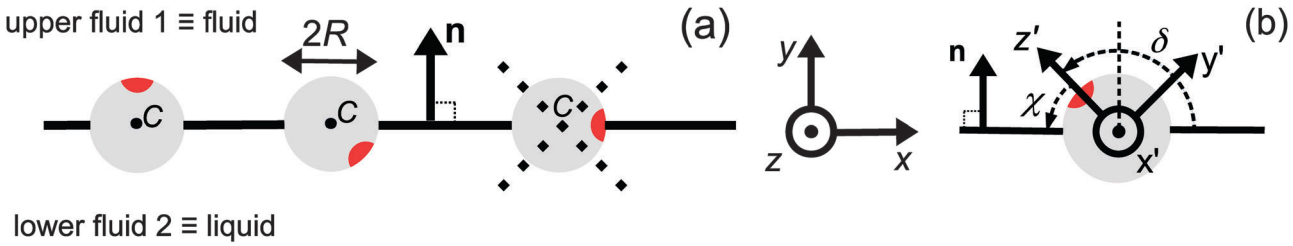

Fig. 1 (a) Typical configurations of an active Janus particle, *i.e.*, a spherical colloid (shown as a gray disk in sidewise projection onto the plane spanned by the symmetry axis of the particle and the interface normal **n**) with a spherical cap providing a catalytic region (red), trapped at the interface (solid black line) between two fluids. The leftmost configuration corresponds to the catalytic cap having a preference for the upper fluid and very strong, effective repulsive interactions between the interface and the catalytic cap. The configuration in the middle corresponds to the catalytic cap exhibiting a preference for the lower fluid and effective interactions between the interface and the catalytic cap, having a long-ranged attractive component and a dominant short-ranged repulsive one. The configuration on the right ("crossed out") does not occur due to the assumed preference of the catalyst for contact with one of the two fluids. In all three configurations C denotes the center of the sphere. (b) The coordinate systems employed to describe the motion of such trapped active Janus colloids are shown at the right. In the spatially fixed unprimed coordinate system the interface normal **n** points into the y-direction, the x-direction is in the plane spanned by **n** and the symmetry axis of the particle, and the unit vector in the z-direction lies in the plane of the interface. The primed coordinate system is co-moving (translating and rotating) with the particle. The origin O′ of the primed coordinate system coincides with the center C of the sphere. The z'- and y'-directions lie in the plane spanned by **n** and the symmetry axis of the particle. The z'-axis passes through the center of the catalytic cap, and the unit vector in the x'-direction lies in the plane of the interface. The angle $\delta \in [\delta_m, \pi - \delta_m) \cup [\pi + \delta_m, 2\pi - \delta_m)$, where $\delta_m < \pi/2$ denotes the value of δ (with the orientation of the cap in the upper fluid, as shown in the figure) at which the rim of the cap touches the interface, gives the orientation of the O′z' direction with respect to Ox, where O is the origin of the fixed coordinate system. The unit vectors of the primed and unprimed coordinate systems are related *via* $\mathbf{e}_{x'} = \mathbf{e}_z$, $\mathbf{e}_{z'} = \cos(\delta)\,\mathbf{e}_x + \sin(\delta)\,\mathbf{e}_y$, and $\mathbf{e}_{y'} = \sin(\delta)\,\mathbf{e}_x - \cos(\delta)\,\mathbf{e}_y$.

recently, induced Maragoni flows can drive the motion of active particles even if they are not trapped at but located nearby the interface.[26])

If none of the reaction products exhibits a preference for the interface, the Marangoni type of propulsion is no longer in action. The question arises if for an active Janus particle, trapped at the interface, sustained motion along the interface can still occur due to the self-induced phoresis mechanism, which works in the bulk solution. For reasons of simplicity, in the following we focus solely on the case of planar interfaces. In thermal equilibrium (*i.e.*, in the absence of diffusiophoresis), a Janus particle trapped at the interface typically exhibits a configuration in which the particle axis is not aligned with the normal of the interface (see Fig. 1). Therefore, at first it seems that, upon "turning on" the chemical reaction, motion along the interface may be achieved.‡ However, it is known that the motion at the interface between two fluids generally involves a coupling between translation and rotation.[2,27,28] Thus the possibility arises that the translation along the interface may lead to a rotation of the axis of the particle towards alignment with the interface normal. Since self-phoresis of active particles is, in general, characterized by very small Reynolds (Re) numbers (*i.e.*, inertia does not play a role),[1,3,8,12] such a rotation of the axis of the particle leads to a motionless state once the axis is aligned with the normal, *i.e.*, the motile state is just a transient. Therefore, predicting whether or not for a particular system sustained motion along the interface may occur *via* self-diffusiophoresis requires an understanding of the interplay between the equilibrium configuration of the Janus particle at the interface, the distribution of reactant and product molecules upon turning on the chemical reaction, and the induced hydrodynamic flows in the liquid and the fluid.

Here we study theoretically the issue of sustained self-diffusiophoresis along a liquid–fluid interface for a simple model of a spherical, chemically active Janus colloid trapped at a liquid–fluid interface. Nonetheless we expect this simple model to qualitatively capture some of the main physical features of the phenomenon. The chemical activity of the particle is modeled *via* the production of one species of solute molecules, with a uniform rate across the catalytic region. We determine the conditions under which this model system exhibits sustained motility. These conditions involve the interplay between the equilibrium configuration, the difference in viscosity between the two adjacent fluids, and the interactions between the particle and the product (solute) molecules. Finally, for particles trapped at the interface we analyze the persistence length and the stability of the motile state against thermal fluctuations and compare it with the corresponding motion in unbound fluids.

2 Model

In this section we discuss our model for a catalytically active, spherical Janus colloid[9] trapped at a liquid–fluid interface (see Fig. 1(a)). The colloid (gray disk in Fig. 1(a)) of radius R has a spherical cap region (the red patch in Fig. 1(a)) decorated by a catalyst which promotes the conversion A → B of "fuel" molecules A into product (solute) molecules B. The particle is trapped at the interface (the horizontal black line in Fig. 1(a))

‡ Even if the equilibrium configuration would correspond to the symmetry axis being aligned with the interface normal, as, *e.g.*, in the case of strongly repulsive, effective interactions between the interface and the catalytic patch, fluctuations will perturb this state of alignment and the previous scenario is recovered. These fluctuations can be thermal fluctuations of the orientation of the axis around the equilibrium position, or non-equilibrium fluctuations of the rate of the catalytic reaction along the surface.

between the two fluids "1" and "2" (denoted also as fluid and liquid, respectively) with bulk viscosities η_1 and η_2, respectively. For simplicity we assume that the fuel (A) and the product (B) molecules diffuse freely in both fluids, that neither of the two species A and B exhibits a preference for either the interface or one of the two fluid phases, and that the concentration of A molecules in the two fluid phases is at a steady state. Furthermore, it is assumed that the fuel molecules A are present in abundance such that their number density is not affected by the reaction. (Under the latter assumption, the dynamics of the fuel molecules is irrelevant and their sole role is, similar to that of the catalyst, that of a "spectator" enabling the reaction due to which active motion emerges. Thus within this model the diffusion constants of the A particles in the two fluids do not enter the description.) Accordingly, we assume that the effects of the chemical reaction can be approximated by representing the catalyst area as an effective source of solute which releases molecules B (at a time independent rate per area of catalyst). We denote the diffusion constants of the solute molecules in the two fluids as D_1 and D_2, respectively.

For a Janus particle trapped at the interface several scenarios can emerge if the parameters controlling the effective particle–interface interactions, such as the coverage by the catalyst or the three-phase contact angle of the "bare" particle (*i.e.*, without catalyst), are changed. Here we restrict the discussion to the case that the particle and the two fluid phases have densities and surface tensions for which the deformations of the interface due to buoyancy are negligible, and we assume that the catalytic cap is completely immersed in one of the two fluid phases. Thus the Janus particle forms the three-phase contact angle of the bare particle.[16] Furthermore, we assume that the effective interaction between the particle and the interface is such that the catalytic cap cannot jut into the other fluid, *i.e.*, the circular boundary between the catalytic cap and the bare regions gets pinned at the three-phase contact line (between fluid 1, fluid 2, and the particle surface) upon touching it. (Accordingly, if the symmetry axis of the particle, *i.e.*, the axis passing through the center C of the particle and the center of the catalytic spherical cap, would rotate beyond this touching point, the interface would no longer be planar.) For simplicity, we further restrict our discussion to the case in which the three-phase contact angle of the bare particle is $\pi/2$, which implies that the catalytic cap has to be smaller than a hemisphere. Actually, the size of the catalytic cap should be sufficiently small so that thermal fluctuations of the orientation around the equilibrium one do not lead to the aforementioned touching, which causes pinning of the liquid–fluid interface. With these assumptions, the center of the Janus particle lies in the plane of the interface. (As it will be discussed in Section 3, this particular configuration significantly simplifies the technical details, and thus provides transparent and physically intuitive results.) The orientation of the symmetry axis is determined by the effective interactions between the catalytic cap and the interface. For net repulsive interactions[16] we expect the equilibrium distribution of the symmetry axis of the particle to be peaked at the direction normal to the interface. If, on the other hand, the effective interaction between the catalytic cap and the interface includes a long-ranged attractive part and a dominant short-ranged repulsive part, the equilibrium distribution is expected to be peaked at a direction which is close to, but distinct from, an orientation parallel to the interface. (Since the catalytic material is assumed to be completely immersed in one of the fluids, a net attractive interaction between the catalytic cap and the interface would be incompatible with our model.)

Since the surface tension compensates any action of the active Janus particle in the direction of the interface normal (which implies that the particle is trapped at the interface), translation of the particle upon turning on the catalytic reaction is possible only within the planar interface. Thus a motile state can be reached only if the axis of the Janus particle is not oriented perpendicular to the interface. Due to the symmetry of the problem, all lateral directions of the particle translation are equivalent; in other words, at a given tilting angle of the symmetry axis with respect to the normal, upon rotating the symmetry axis around the normal a state of motion emerges which is identical to the one in the original configuration. This allows us to consider the particle motion in the plane spanned by the axis of the particle (in its orientation at the moment when the catalytic reaction is turned on) and the normal of the planar interface. Thus we neglect the effects of thermal fluctuations leading to a rotation of the axis of symmetry out of this plane. Under this assumption, and in accordance with Fig. 1(b), we choose the coordinate system with the y-axis along the interface normal, pointing towards the upper fluid, the x-axis as the intersection of the interface with the plane of motion, and the z-axis as the normal of the latter (see Fig. 1(b)). For future reference, we also introduce a system of coordinates – with the origin O′ at the center C of the particle and co-moving with the particle –, which is denoted by primed quantities. As shown in Fig. 1(b), in the plane spanned by the axis of symmetry and the normal to the interface passing through the center of the particle we choose the z'-axis to point through the center of the catalytic cap and the x'-axis to lie in the plane of the interface and to be parallel to the z-axis. (These choices for the primed and unprimed coordinates are taken as to facilitate more convenient calculations in Sections 3 and 4 below.)

A viscosity contrast between the two fluids forming the interface leads to the onset of net torques on particles translating along the interface. Therefore the orientation of the symmetry axis of the trapped Janus particle relative to the y-axis will change once the chemical reaction is turned on and the particle is set into translation. Depending on the viscosity contrast between the two fluids, a small fluctuation of the orientation of the symmetry axis can be either amplified by the induced torque, leading to a different, yet motile, state, or suppressed. In the former case the steady state orientation of the axis of the Janus particle is ultimately determined by the geometry of the particle including the shape of the catalytic patch and the details of the effective interactions between the catalytic cap and the interface, which is a complex problem. Here we shall assume that the motion is quasi-adiabatic, in the sense that the rotation of the particle is much slower than the time it takes for the distribution of

solute molecules B and for the flow of the solution to reach a quasi-steady-state corresponding to the instantaneous orientation of the particle. Thus we focus solely on sustained motile states. The determination of the steady-state orientation of the symmetry axis of the particle (which, as noted above, ultimately involves the details of the effective interaction between the catalytic cap and the interface) is left to future research.

As discussed above, the rotations (spinning) of the particle around the symmetry axis are neither contributing to, nor being induced by, the motility along the interface, whereas the rotations of the symmetry axis around the interface normal have the sole effect of changing the direction of the in-plane translation. Therefore describing the motion of the particle at the interface requires only to account for one translational velocity component U_x and one angular velocity component Ω_z corresponding to translation along the x-axis and rotation around the z-axis, respectively. These will be determined by assuming the motion of the fluids to be described by the Stokes equations and the translation and rotation of the particle to be quasi-adiabatic in the sense that the hydrodynamics obeys the (steady state) Stokes equations at the instantaneous state, *i.e.*, the orientation and velocity, of the particle. Finally, we assume that the interface exerts no force on the particle when it is translating along the interface, that the torques exerted by the interface with respect to rotations of the particle around the z-axis are vanishingly small, and that the eventual, small deformations of the interface in the contact line region accompanying such a motion also have negligibly small effects.

The assumption of negligible torques deserves further consideration. In fact, if the catalytic cap leaves its equilibrium orientation, a torque will arise due to the effective interaction between the catalytic cap and the interface. Here we focus our attention on the case in which such contributions are negligible.§ Furthermore, the rotation around the x'-axis involves a moving contact line, which is a well-known conceptual issue in classical hydrodynamics.[29,30] Here we do not attempt to provide a mechanism through which the associated contact line singularity (*i.e.*, translation of the contact line while at the same time the fluids fulfill the no-slip boundary condition) is removed and motion occurs (see, *e.g.*, ref. 31–33). Instead we assume that the region, where a microscopic description is necessary, is very small compared to the typical length scales in the system and that there the expected macroscopic velocity values provide a smooth interpolation.

3 Translational and angular velocities of Janus particles at liquid–fluid interfaces

In order to calculate the angular and translational velocity of Janus particles trapped at a liquid–fluid interface, we model the two immiscible fluids separated by a planar interface as having a continuous, but steeply varying, viscosity profile $\eta(y)$ interpolating between η_2 at $y = -\infty$ and η_1 at $y = +\infty$ across the plane $y = 0$ (compare Fig. 1):

$$\eta(y) = \eta_0 + \frac{\Delta\eta}{2}\tanh\left(\frac{y}{\xi}\right), \tag{1}$$

where $\eta_0 = (\eta_1 + \eta_2)/2$ and $\Delta\eta = \eta_1 - \eta_2$ denote the mean viscosity $\eta_0 = \eta(0)$ and the viscosity contrast $\Delta\eta$, respectively, while ξ, which is of molecular size, characterizes the width of the interface. In the following we consider the case of a vanishingly thin interface, *i.e.*, we take $\xi \to 0$.

3.1 Reciprocal theorem for a particle at liquid–fluid interfaces

We exploit the reciprocal theorem,[24,27,34] derived first by Lorentz[35] (the English translation of the original paper is provided in ref. 36) for the case of a homogeneous fluid and later extended by Brenner[27] to the case in which the viscosity of the fluid varies spatially.¶ The reciprocal theorem states that in the absence of volume forces any two incompressible flow fields $\mathbf{u}(\mathbf{r})$ and $\hat{\mathbf{u}}(\mathbf{r})$, which are distinct solutions of the Stokes equations within the same domain $\mathscr{D}$, *i.e.*, solutions subject to different boundary conditions but on the very same boundaries $\partial\mathscr{D}$, obey the relation

$$\int_{\partial\mathscr{D}} \mathbf{u}\cdot\hat{\boldsymbol{\sigma}}\cdot\mathbf{n}\mathrm{d}S = \int_{\partial\mathscr{D}} \hat{\mathbf{u}}\cdot\boldsymbol{\sigma}\cdot\mathbf{n}\mathrm{d}S, \tag{2}$$

where $\boldsymbol{\sigma}$ and $\hat{\boldsymbol{\sigma}}$ denote the stress tensors corresponding to the two flow fields.

For our system, the assumption of immiscibility of the two fluids translates into the kinematic boundary condition that the velocity components of the flow fields above and below the interface along the direction of the normal to the interface must vanish at the interface. This effectively enforces the interface as a physical boundary across which, concerning the hydrodynamics, there is momentum transfer but no mass transfer. Therefore it is necessary that the hydrodynamic flow is obtained by solving the Stokes equations in the domains above ($\mathscr{D}_1$) and below ($\mathscr{D}_2$) the interface and by subsequently working out the problem by connecting the solutions corresponding to the upper and lower fluids *via* appropriate boundary conditions at the interface (see below). $\mathscr{D}_1$ is delimited by that part $\Sigma_{\mathrm{p}1}$ of the particle surface Σ_{p} exposed to the upper fluid, the surface of the fluid at infinity in the half-plane $y > 0$, and the upper part, $y = 0^+$, of the fluid interface Γ (note that this is the plane with $y = 0$ and less area occupied by the particle); $\mathscr{D}_2$ is defined similarly.‖ We note that the inner normals of the upper ($\mathbf{n}_1$) and lower ($\mathbf{n}_2$) parts of the interface Γ are $\mathbf{n}_1 = \mathbf{e}_y = -\mathbf{n}_2$.

§ Since the typical effective forces between the interface and the catalytic cap decay rapidly with the distance from the interface, the assumption remains valid as long as the catalytic cap is not very close to the interface.

¶ A recent extension of this version of the reciprocal theorem to the case of a free interface, in which the viscosity exhibits an abrupt change across the liquid–air interface, can be found in ref. 24.

‖ Formally, the domains $\mathscr{D}_1$ and $\mathscr{D}_2$ as well as the interface Γ could be closed along the O_x direction by assuming periodic boundary conditions at $|x| \to \infty$; alternatively, one may choose for the surface at infinity, which is closing the domains $\mathscr{D}_1$ and $\mathscr{D}_2$, a spherical one, centered at C and with a radius $R_\infty \to \infty$.

We restrict the discussion to the case in which for both flow fields (*i.e.*, the un-hatted and the hatted one, which are to be considered in the reciprocal theorem), there are no (*e.g.*, externally imposed, or due to surface tension gradients) tangential stresses at the interface. For both the un-hatted and the hatted flow fields, the corresponding flow velocities and stress tensors within the upper and lower domains, which are connected *via* the boundary conditions they have to obey at the interface, are denoted by the indices "1" and "2", respectively. By (i) applying the reciprocal theorem (eqn (2)) in each of the domains $\mathscr{D}_1$ and $\mathscr{D}_2$ (which can be done because Γ is a physical boundary at which the boundary conditions are formally prescribed by imposing the tangential velocity and the stress tensor to take the values given by the (yet unknown) velocity and stress tensor on the other side of the interface, respectively), (ii) adding the left and right hand sides of the two results of applying the reciprocal theorem in $\mathscr{D}_1$ and $\mathscr{D}_2$, (iii) noting that for flow fields, which decay sufficiently fast with the distance from the particle (which typically is the case), the contribution from the integrals over the surfaces at infinity are vanishingly small, (iv) using the relation (see above) $\mathbf{n}_1 = -\mathbf{n}_2 = \mathbf{e}_y$ between the interface normals, and (v) noting that the boundary conditions for the flow velocity at the interface Γ impose zero normal components, *i.e.*, $(\mathbf{u}_1\cdot\mathbf{e}_y)|_{y=0} = 0$, $(\mathbf{u}_2\cdot\mathbf{e}_y|)_{y=0} = 0$ and continuous tangential components[27] so that $\mathbf{u}_1|_{y=0_+} = \mathbf{u}_2|_{y=0_-} =: u_{||}\mathbf{e}_{||}$ (with similar relations for the hatted velocity field), where $\mathbf{e}_{||}\cdot\mathbf{e}_y = 0$, we arrive at

$$\int_\Gamma \left(u_{||}\mathbf{e}_{||}\right)\cdot(\hat{\boldsymbol{\sigma}}_1 - \hat{\boldsymbol{\sigma}}_2)|_{y=0}\cdot\mathbf{e}_y \mathrm{d}S + \int_{\Sigma_\mathrm{p}} \mathbf{u}\cdot\hat{\boldsymbol{\sigma}}\cdot\mathbf{n}\mathrm{d}S = \int_\Gamma \left(\hat{u}_{||}\mathbf{e}_{||}\right)\cdot(\boldsymbol{\sigma}_1 - \boldsymbol{\sigma}_2)|_{y=0}\cdot\mathbf{e}_y \mathrm{d}S + \int_{\Sigma_\mathrm{p}} \mathbf{u}\cdot\hat{\boldsymbol{\sigma}}\cdot\mathbf{n}\mathrm{d}S. \tag{3}$$

In the absence of tangential stresses at the interface the difference of normal stresses at the interface $(\boldsymbol{\sigma}_1 - \boldsymbol{\sigma}_2)|_{y=0}\cdot\mathbf{e}_y$ is the force corresponding to the Laplace pressure,[27] and thus is a vector oriented along the normal $\mathbf{e}_y$ of the interface. Therefore the first integral on the left hand side of eqn (3) vanishes due to $\mathbf{e}_{||}\perp\mathbf{e}_y$. By a similar argument, the first integral on the right hand side of eqn (3) vanishes, too. Thus for the present system the reciprocal theorem takes the simple form given in eqn (2) but with $\mathscr{D}$ replaced by Σ_p.

In order to determine the translational and the angular velocity of the Janus particle, we shall select an appropriate set of "dual problems" (the "hatted" quantities), typically associated with known solutions for spatially uniform translations or rotations (under the action of external forces or torques) of solid spheres with prescribed boundary conditions at their surfaces. To this end we consider a solid sphere of radius R with no-slip boundary conditions translating with velocity $\hat{\mathbf{U}}$ and rotating with angular velocity $\hat{\boldsymbol{\Omega}}$ under the action of the external force $\hat{\mathbf{F}}$ and the external torque $\hat{\mathbf{L}}$. At the surface of the particle, the flow $\hat{\mathbf{u}}(\mathbf{r}_\mathrm{p})$, where $\mathbf{r}_\mathrm{p}$ denotes a point at the particle surface Σ_p, is given by

$$\hat{\mathbf{u}}(\mathbf{r}_\mathrm{p}) = \hat{\mathbf{U}} + \hat{\boldsymbol{\Omega}}\times(\mathbf{r}_\mathrm{p} - \mathbf{r}_\mathrm{c}), \tag{4}$$

where $\mathbf{r}_\mathrm{C}$ is the position of the center C of the sphere. (Both $\mathbf{r}_\mathrm{p}$ and $\mathbf{r}_\mathrm{C}$ are measured from a common, arbitrary origin, the location of which drops out from $\mathbf{r}_\mathrm{p} - \mathbf{r}_\mathrm{C}$.) Similarly, we consider a Janus particle, which translates with velocity $\mathbf{U} = U_x\mathbf{e}_x$ and rotates with an angular velocity $\boldsymbol{\Omega} = \Omega_z\mathbf{e}_z$ around the axis, which is parallel to O_z and passes through the moving center C of the particle at its instantaneous position. If the particle exhibits boundary conditions given by a phoretic slip velocity $\mathbf{v}(\mathbf{r}_\mathrm{p})$, the flow $\mathbf{u}(\mathbf{r}_\mathrm{p})$ at its surface is given by

$$\mathbf{u}(\mathbf{r}_\mathrm{p}) = \mathbf{U} + \boldsymbol{\Omega}\times(\mathbf{r}_\mathrm{p} - \mathbf{r}_\mathrm{C}) + \mathbf{v}(\mathbf{r}_\mathrm{p}). \tag{5}$$

By using eqn (4) and noting that $\hat{\mathbf{U}}$ and $\hat{\Omega}_z$ are spatially constant vectors, the right hand side (rhs) of eqn (2) can be re-written as

$$\int_{\Sigma_\mathrm{p}} \hat{\mathbf{u}}\cdot\boldsymbol{\sigma}\cdot\mathbf{n}\mathrm{d}S = \hat{\mathbf{U}}\cdot\mathbf{F} + \hat{\boldsymbol{\Omega}}\cdot\mathbf{L}, \tag{6}$$

where $\mathbf{F} = \int_{\Sigma_\mathrm{p}}\boldsymbol{\sigma}\cdot\mathbf{n}\mathrm{d}S$ and $\mathbf{L} = \int_{\Sigma_\mathrm{p}}(\mathbf{r}_\mathrm{p} - \mathbf{r}_\mathrm{C})\times\boldsymbol{\sigma}\cdot\mathbf{n}\mathrm{d}S$ denote the force and the torque, respectively, experienced by the Janus particle. (In eqn (6), $\mathbf{n}$ denotes the normal of the surface Σ_p of the particle, oriented into the fluid.) We note that while the active motion of Janus particles in the bulk is force- and torque-free, this is, in general, not the case if the motion occurs at the interface because the interface can exert forces and torques on the particle. However, because we have assumed that the interface does not exert a force in the case of translations of the Janus particle along the interface or a torque in the case of rotations around the z-axis (in the sense of spinning around an axis parallel to the z-axis, as discussed above), the components F_x and L_z vanish. Therefore, if the reciprocal problem involves only translations along the x-axis and/or such rotations around the z-axis, the rhs of eqn (6), and, consequently, of eqn (2) is zero. Restricting now the dual problem as discussed above to such a choice, and using eqn (5) for the left hand side of eqn (2), we arrive at

$$U_x\hat{F}_x + \Omega_z\hat{L}_z = -\int_{\Sigma_\mathrm{p}}\mathbf{v}(\mathbf{r}_\mathrm{p})\cdot\hat{\boldsymbol{\sigma}}\cdot\mathbf{n}\mathrm{d}S. \tag{7}$$

3.2 Calculation of the translational and angular velocities

We proceed by selecting two so-called dual problems, each involving only one of the two types of motions (translation or rotation only) for both of which eqn (7) holds. These will provide two relations allowing one to determine U_x and Ω_z. The first one, denoted by the index "1", is that of a sphere of radius R, the center of which lies in the plane of the flat, sharp ($\xi \to 0$) liquid–fluid interface (see eqn (1)), translating without rotation with velocity $\hat{\mathbf{U}} = \hat{U}_x\mathbf{e}_x$ along the interface. This problem has been solved analytically,[28] and the result of interest here is

$$(\mathbf{n}\cdot\hat{\boldsymbol{\sigma}}_1)|_{\Sigma_\mathrm{p}} = -\frac{3}{2R}\eta(\mathbf{r}_\mathrm{p})\hat{\mathbf{U}}. \tag{8}$$

This leads to (see Appendix A for the details of the calculation)

$$\hat{F}_{1x} = -6\pi R\eta_0\hat{U}_x := \alpha_1\hat{U}_x \tag{9a}$$

and

$$\hat{L}_{1z} = +\frac{3\pi}{2}R^2\Delta\eta\hat{U}_x := \beta_1\hat{U}_x. \tag{9b}$$

After inserting eqn (8) and (9) into eqn (7) and canceling the common factor $\hat{U}_x$, we obtain

$$\alpha_1 U_x + \beta_1 \Omega_z = C_1 := \frac{3}{2R}\int_{\Sigma_p} \eta(\mathbf{r}_p) v_x(\mathbf{r}_p) \mathrm{d}S \tag{10}$$

where $v_x(\mathbf{r}_p)$ is the x-component of the phoretic slip velocity at the point $\mathbf{r}_p$ on the surface of the particle.

The second problem which we consider, denoted by the index "2", is that of the driven rotation, without translation, with angular velocity $\hat{\mathbf{\Omega}} = \hat{\Omega}_z \mathbf{e}_z$ of a spherical particle of radius R, the center of which lies in the plane of the flat, sharp ($\xi \to 0$) liquid–fluid interface. As noted before, this is a more involved problem due to the concomitant issue of contact line motion. For the case in which one of the two fluids has a vanishingly small viscosity, an exact solution was constructed in ref. 33 under the assumption that a slip boundary condition, with a spatially uniform slip length along the surface, applies across that surface region which is immersed in the fluid of non-vanishing viscosity, called liquid. The result of this calculation shows that for typical slip lengths l_0, which are much smaller than the size of the particle,** at distances $|y|/l_0 \gg 1$ from the interface the hydrodynamic flow within the liquid is *de facto* identical to the one which would have occurred if the rotating sphere would have been completely immersed in the liquid and a no-slip boundary condition would have been applied. Thus in this context the only role played by the slip is to remove the contact line singularity, as discussed in Section 2. This can be interpreted in the sense that the same solution would emerge if one assumes that the fluid slips only in a narrow region localized close to the three-phase contact line, while the no-slip condition holds for the rest of the sphere. This view is confirmed by an alternative solution presented in ref. 38 for the same problem of the rotation of a sphere at the interface between a liquid and a fluid of vanishing viscosity.

In the following we shall adopt the latter interpretation and make the ansatz that for our above problem "2" (in which the viscosities of both fluids are, in general, certain non-zero quantities) with a sharp interface ($\xi \to 0$) the expression for the stress tensor at the surface of the particle is given by the one in ref. 33, *i.e.*,

$$(\mathbf{n} \cdot \hat{\boldsymbol{\sigma}}_2)|_{\Sigma_p} = -3\eta(\mathbf{r}_p)\hat{\Omega}_z(\mathbf{e}_z \times \mathbf{n})|_{\Sigma_p}, \tag{11}$$

except for a small region localized close to the three-phase contact line. As noted, the expression above is expected to provide a reliable approximation if the viscosity contrast between the two fluids is large.[33] In the limiting case of the two fluids becoming identical, by construction eqn (11) reduces to the exact result corresponding to a sphere rotating without slip in a spatially homogeneous fluid.

With the assumption that the small region near the three-phase contact line contributes negligibly to the integrals over the surface of the particle, eqn (11) implies that the corresponding components of the forces and torques required for the reciprocal theorem (eqn (7)) are given by (see Appendix A)

$$\hat{F}_{2x} \simeq +3\pi R^2 \Delta\eta \hat{\Omega}_z := \alpha_2 R \hat{\Omega}_z \tag{12a}$$

and

$$\hat{L}_{2z} \simeq -8\pi\eta_0 R^3 \hat{\Omega}_z := \beta_2 R \hat{\Omega}_z. \tag{12b}$$

After inserting eqn (11) and (12) into eqn (7) and canceling the common factor $\hat{\Omega}_z$, we obtain

$$\alpha_2 U_x + \beta_2 \Omega_z = C_2 := \frac{3}{R}\int_{\Sigma_p} \eta(\mathbf{r}_p)\big(\mathbf{n} \times \mathbf{v}(\mathbf{r}_p)\big)_z \mathrm{d}S. \tag{13}$$

Once a particular model is given for the mechanism through which the chemical activity determines the phoretic slip $\mathbf{v}(\mathbf{r}_p)$, the quantities C_1 and C_2 can be computed and U_x and Ω_z follow from eqn (10) and (13). This concludes the calculation of the translational (U_x) and angular (Ω_z) velocities of the Janus particle trapped at the interface. We note that in the limit $\Delta\eta \to 0$ eqn (10) and (13) reduce to the corresponding components for a Janus particle moving in a homogeneous fluid,[34] *i.e.*, $U_x = -\frac{1}{4\pi R^2}\int_{\Sigma_p} v_x \mathrm{d}S$ and $\Omega_z = -\frac{3}{8\pi R^3}\int_{\Sigma_p}(\mathbf{n} \times \mathbf{v})_z \mathrm{d}S$, respectively.

The latter result deserves further consideration. In the case of translation along the interface, in the limit $\Delta\eta \to 0$ the recovery of the result corresponding to a particle moving in a homogeneous fluid is to be expected in the case of a particle having its center located at the interface. This is so, because the flow around the Janus particle translating at the interface converges, as the viscosity contrast approaches zero, towards the solution corresponding to the motion in a homogeneous fluid.†† On the other hand, this expectation does not hold in the case of rotation: the immiscibility of the fluids requires that the interface modifies the flow by "forcing" the fluid to flow along the interface. This different structure of the flow survives even if the viscosity contrast is vanishing. Therefore, recovering nonetheless the result for rotation in a homogeneous fluid simply means that the ansatz for the stress tensor at the surface of the particle (eqn (11)) renders the correct limiting behavior for vanishing viscosity contrast, irrespective of the corrections provided by the presence of the interface.

4 Results and discussion

Solving eqn (10) and (13) for U_x and Ω_z leads to

$$U_x = \frac{C_1\beta_2 - \beta_1 C_2}{\alpha_1\beta_2 - \alpha_2\beta_1} \tag{14a}$$

** For example, for water on PDMS or on glass surfaces the estimated slip length l_0 is well below 100 nm.[37]

†† In the case of a homogeneous fluid the flow around the particle which translates is symmetric with respect to any plane containing the translation direction. Thus the flow is characterized by a vanishing velocity normal to such a symmetry plane and a continuous velocity tangential to that symmetry plane (which thus can be regarded as an "imaginary planar interface" where the kinematic boundary conditions of an actual interface between immiscible liquids are obeyed).

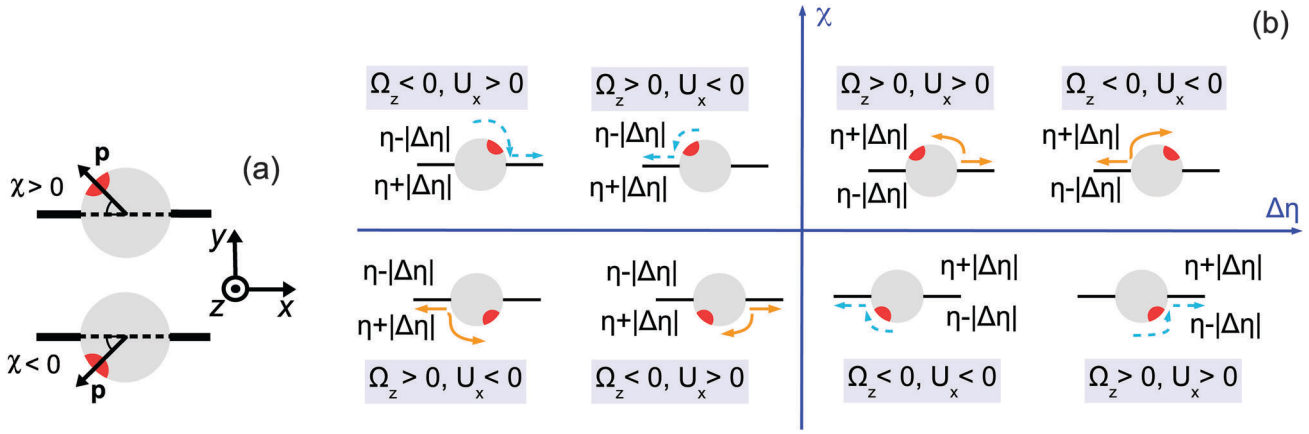

Fig. 2 (a) Definition of the director orientation with respect to the interface. (b) Schematic diagram indicating the configurations of sustained motility as a function of the viscosity contrast $\Delta\eta = \eta_1 - \eta_2$ and the position of the active cap (red) with respect to the interface (black) given by the acute angle χ between the director and the interface. The orange and blue colors of the arrows refer to repulsive and attractive interactions between the chemically generated solute and the particle, respectively. In each case we have illustrated both the situation in which the catalytic cap is tilted to the left and the situation in which it is tilted to the right of the interface normal $\mathbf{e}_y$, respectively. This change in the tilting of the cap amounts to all blue and orange arrows turning around and pointing into opposite directions but without changing colors because the stability criterion ($\mathrm{sign}(U_x/(R\Omega_z))$) is invariant with respect to this change. Therefore in each quadrant only either the repulsive or the attractive interaction case is associated with sustained motion.

and

$$\Omega_z = \frac{\alpha_1 C_2 - C_1 \alpha_2}{\alpha_1 \beta_2 - \alpha_2 \beta_1}. \tag{14b}$$

For the discussion of these results we find it more convenient to employ the following alternative description of the orientation of the particle with respect to the interface. We define the director $\mathbf{p}$ of the Janus particle as being the unit vector corresponding to the axis of symmetry of the Janus particle oriented towards the catalytic cap. The acute angle between the director and the interface, in the plane (xOy), is denoted as χ (Fig. 2(a)). It is defined as a signed quantity, with the sign convention that χ is positive if $\mathbf{p}$ points towards the half-space $y > 0$ and negative otherwise; thus $-\pi/2 \leq \chi \leq \pi/2$. (The angle χ is thus connected with δ (see Fig. 1(b)) *via* $\chi = \min(\delta,\pi - \delta)$, if $0 < \delta < \pi$, and $\chi = -\min(\delta - \pi,2\pi - \delta)$, if $\pi < \delta < 2\pi$.) The states with $\chi = \pm\pi/2$ correspond to the director being parallel and antiparallel, respectively, to the interface normal $\mathbf{e}_y$, for which U_x vanishes. Therefore, in order for a state of motion along the surface, *i.e.*, $U_x \neq 0$, to be sustainable, any change in χ occurring as a result of motion along the interface should be such that $|\chi|$ decreases (*i.e.*, the director rotates towards the interface).

4.1 Configurations of sustained motility

Referring now to Fig. 2(b) and considering as an example the situation shown in the upper part with the catalytic cap tilted slightly to the left of the normal $\mathbf{e}_y$, for which $\chi > 0$, one infers that, upon turning on the chemical reaction, for repulsive (attractive) interactions between the solute (*i.e.*, the reaction products) and the particle, the latter will tend to move towards the right (left), so that $U_x > 0$ ($U_x < 0$). If $\Delta\eta > 0$, *i.e.*, the upper fluid is more viscous than the lower one, translation with $U_x > 0$ gives rise to a torque on the particle which induces a counterclockwise rotation, *i.e.*, $\Omega_z > 0$. (The upper part of the particle experiences a stronger retarding friction than the lower part of the particle.) This corresponds to a decrease of χ towards zero and thus promotes motility. This situation is shown in the right upper quadrant of Fig. 2(b). On the other hand, translation with $U_x < 0$ (and still for $\chi > 0$ as well as the cap tilted to the left of the interface normal; not shown in the right upper quadrant of Fig. 2(b)) gives rise to a clockwise rotation (*i.e.*, $\Omega_z < 0$, for the same reason as above) and therefore to an increase of χ towards $\pi/2$, *i.e.*, rotation opposes motility. If $\Delta\eta < 0$ (and still $\chi > 0$ with the cap tilted to the left of the interface normal), the sign of those torques (which are described by the same color), and thus of the corresponding angular velocities, is reversed. In this case, the translation towards the left ($U_x < 0$) is accompanied by a rotation which decreases χ (*i.e.*, $\Omega_z > 0$) and thus promotes motility (see the left upper quadrant of Fig. 2(b)), while translation towards the right (*i.e.*, $U_x > 0$ and still $\chi > 0$ with the cap tilted to the left of the interface normal; not shown in the left upper quadrant) is opposed by the rotation of the director. Following the above reasoning for the various possible configurations (*i.e.*, catalytic cap above or below the interface, attractive or repulsive solute–particle interactions, and viscosity contrast positive or negative), in the plane ($\Delta\eta$,χ) one can identify the cases in which sustained motion would occur, depending on the repulsive or attractive character of the interactions between the solute and the particle. These configurations are summarized in Fig. 2(b), where the arrows indicate the corresponding directions of the translation and rotation. The colors blue and orange of the arrows refer to repulsive and attractive interactions, respectively.

From the discussion above (see also the schematic diagram in Fig. 2(b)) one infers that the states with sustained motion must satisfy $U_x/(R\Omega_z) > 0$ for $\Delta\eta > 0$ or $U_x/(R\Omega_z) < 0$ for $\Delta\eta < 0$. Therefore, for a given system these signs of $U_x/(R\Omega_z)$ as a function of the viscosity contrast $\Delta\eta$ provide necessary conditions

for the occurrence of such motile states. However, in order to explicitly calculate the sign of the ratio $U_x/(\Omega_z R)$ one needs to provide an explicit form for $\mathbf{v}_s(\mathbf{r}_p)$ which determines U_x and Ω_z (eqn (10), (13) and (14)). In order to determine $\mathbf{v}_s(\mathbf{r}_p)$ it is in principle necessary (i) to specify the geometrical properties of the catalytic cap responsible for the reaction within the fluids; (ii) to specify the reaction; (iii) to provide the diffusion constants of the reactant and product molecules in the two fluids (for example, they can either diffuse in both fluids but with different diffusion constants, or some of the reactants or products may effectively be confined to one of the two fluids), as well as any effective interaction between these molecules and the interface (*e.g.*, whether or not they act as surfactants); (iv) to provide the interaction potentials of the various molecular species in the two solutions (*i.e.*, the two fluids plus the reactants and the products) with the Janus particle as a whole as well as with its surface (for both the catalyst covered part and the inert part).

4.2 Motility of a model chemically active Janus colloid at fluid interfaces

Here we focus on the simple model of a chemically active Janus particle as introduced in Section 2, for which there is only a single reaction product ("solute") diffusing in both fluids and for which the reactant molecules are present in abundance and diffusing very fast in both fluids, such that in both fluids the number density of reactant molecules is *de facto* time-independent and spatially uniform. The effective interaction of the solute with the colloidal particle is assumed to be of a range which is much smaller than the radius R of the colloid and to be similar for the catalyst-covered part and the inert part of the colloid. Furthermore, we assume a sharp interface (*i.e.*, $\xi \to 0$ so that $\eta(\mathbf{r}_p) = \eta(y)$ with $\eta(y) = \eta_1$ for $y > 0$, while $\eta(y) = \eta_2$ for $y < 0$). The latter assumptions imply that, by adopting the classical theory of phoresis[8,9,13] which has been developed for homogeneous (*i.e.*, constant viscosity) fluids, one can express the phoretic slip as being proportional to the solute concentration gradient along the surface at all points of the surface of the particle except for a small region near the interface. Within the corresponding proportionality factor $\mathscr{L}/(\beta\eta)$ (the so-called "phoretic mobility"; see, *cf.*, eqn (20)), where $\beta = 1/(k_B T)$, k_B is the Boltzmann constant, and T denotes the absolute temperature, it is possible to identify the contribution $\mathscr{U}(h)$ of the solute–particle interaction (relative to the solvent–particle interaction). $\mathscr{U}(h)$ is encoded in $\mathscr{L}$ (which has the units of an area) according to[8]

$$\mathscr{L} = \int_0^\infty \mathrm{d}h h\left(\mathrm{e}^{-\beta\mathscr{U}(h)} - 1\right), \tag{15}$$

where h is the distance between the point-like solute and the particle surface. The potential $\mathscr{U}(h)$ is assumed to be such that $\mathscr{U}(h \to 0) = +\infty$, *i.e.*, right at the particle surface the solvent is strongly preferred. The potential can be either repulsive at all distances, or it can become attractive beyond a certain distance h_0 (and thus has to have an attractive minimum because at large distances it decays to zero); the latter case corresponds to the adsorption of the solute. Note that $\mathscr{L} < 0$ for purely repulsive interactions $\mathscr{U}(h)$, while if $\mathscr{U}(h)$ has an attractive part and h_0 is sufficiently small, one has $\mathscr{L} > 0$. In the following, the notion of "attractive interactions" will refer strictly to the latter case, *i.e.*, potentials $\mathscr{U}(h)$ which have attractive parts and satisfy $\mathscr{L} > 0$. At this stage we do not yet particularize the cap to more than the assumed spherical cap shape and to being completely immersed into one of the two fluids.

Under the above assumptions, the phoretic slip $\mathbf{v}(\mathbf{r}_p)$ follows from the solute distribution around the surface of the Janus particle. We further assume that the diffusivity $D(\mathbf{r})$ of the solute molecules is sufficiently high such that the number density distribution $\rho(\mathbf{r},t)$ of the solute is not affected by the convection of the fluids (*i.e.*, we assume that the Péclet number Pe is small) and that a steady state distribution $\rho(\mathbf{r})$ of solute is established at timescales which are much shorter than the characteristic translation time R/U_x of the colloid. With this, $\rho(\mathbf{r})$ obeys the diffusion equation

$$\nabla\cdot[D\nabla\rho] = 0 \tag{16}$$

subject to the boundary conditions

$$\lim_{r\to\infty}\rho = 0, \quad -D\nabla\rho\cdot\mathbf{n}|_{r=R} = QH(\theta_0 - \theta), \tag{17}$$

where $\mathbf{n}$ is the outer normal of the particle, Q denotes the number of solute molecules generated per area and per time at the location of the catalytic cap, and $H(x)$ is the Heaviside step function ($H(x > 0) = 1$, $H(x < 0) = 0$). (In accordance with the assumptions of the model (see Section 2), in the above diffusion equation there are no terms to account for eventual interactions of the solute with the interface or with external fields.)

Since actually only the distribution of solute at the particle surface is required in order to calculate the phoretic slip, instead of seeking for the full solution $\rho(\mathbf{r})$ of eqn (16), which is a difficult problem, we only focus on the solute distribution at the particle surface. In the co-moving (primed) coordinate system (see Fig. 1(b)), in which the phoretic slip velocity is most conveniently calculated, we introduce, in the usual manner, the common spherical coordinates (r', θ', ϕ') defined *via*

$$\begin{aligned} x' &= r'\sin(\theta')\cos(\phi') \\ y' &= r'\sin(\theta')\sin(\phi') \\ z' &= r'\cos(\theta'). \end{aligned} \tag{18}$$

Accordingly, the solute distribution at the particle surface $\rho(\mathbf{r}'_P) = \rho(R,\theta',\phi')$ can be expressed as a series expansion in terms of the spherical harmonics $Y_{\ell m}(\theta',\phi')$:[39]

$$\rho(R,\theta',\phi') = \sum_{\ell=0}^{\infty}\sum_{m=-\ell}^{m=\ell} A_{\ell,m}Y_{\ell m}(\theta',\phi'), \tag{19}$$

where the coefficients $A_{\ell m}$ are functions of the radius R and of the other parameters (temperature, diffusion constants, viscosities, rate of solute production, *etc.*) characterizing the system. In the co-moving system, the phoretic slip can be

expressed in terms of the gradients of $\rho(\mathbf{r}'_P)$ along the surface of the particle[5,8,9,13] (except at the three-phase contact line):

$$\mathbf{v}(\mathbf{r}'_P) = -\frac{\mathscr{L}}{\beta\eta(\mathbf{r}_P)}\nabla_{||}{}'\rho(\mathbf{r}'_P) := v_{\theta'}\mathbf{e}_{\theta'} + v_{\phi'}\mathbf{e}_{\phi'} \tag{20}$$

where $\nabla_{||}{}' = \frac{1}{R}\mathbf{e}_{\theta'}\partial_{\theta'} + \frac{1}{R\sin\theta'}\mathbf{e}_{\phi'}\partial_{\phi'}$ denotes the projection of the gradient operator along the surface of the particle.

In order to determine the x-component v_x of the slip-velocity in the spatially fixed coordinate system, we use eqn (19) and (20) and employ the relationship between the unit vectors of the spatially fixed coordinate system and the co-moving one (see Fig. 1(b)). Knowledge of v_x allows one to determine the quantities C_1 and C_2 introduced in eqn (10) and (13) (see Appendix B for details):

$$C_1 = -2\sqrt{3\pi}\frac{\mathscr{L}\cos(\delta)}{\beta}A_{1,0}, \tag{21}$$

and

$$C_2 = 0. \tag{22}$$

It is interesting to note that, apart from materials properties ($\mathscr{L}$) and temperature, C_1 depends solely on the projection ($\cos(\delta)$) of the particle director onto the plane of the interface and on the real amplitude $A_{1,0}$ (see eqn (19)) of $Y_{10}(\theta',\phi') = \sqrt{3/(4\pi)}\cos(\theta')$. This is that contribution to the angular dependence of ρ along the particle surface which varies slowest between the poles at $\theta' = 0$ (center of the cap) and $\theta' = \pi$. This can be interpreted as an indication that for the model considered here the difference in the solute density between that at the catalytic pole and at the inert antipole is the dominant characteristics while the details of the variation of the density along the surface between these two values are basically irrelevant for the motion of the particle.

In the case that the two fluids have the same viscosity, *i.e.*, $\Delta\eta = 0$, and the diffusion constant for the product molecules is the same in the two fluids (*e.g.*, being related to the viscosity *via* the Stokes–Einstein relation), for the model considered here, according to which the reactant and product molecules can diffuse freely in both fluids and unhindered by the interface, the diffusion equation (eqn (16) and (17)) becomes identical to the one in a homogeneous bulk fluid which can be solved analytically.[9,13] (Thus, in this limit there is no signature of the interface left in the diffusion problem.) The corresponding expansion into spherical harmonics of the solute density at the surface of the particle (for a bulk solvent without an interface) leads to the expression

$$A^{(b)}_{1,0} = \kappa\frac{QR}{D_0}, \tag{23}$$

where κ is a dimensionless factor determined by the geometry of the Janus sphere (*i.e.*, the extent of the catalyst covered area) and D_0 is the diffusion constant of the product molecules in the fluids of viscosities $\eta_1 = \eta_2 = \eta_0$. This leads to the ansatz

$$A_{1,0} = \varsigma(\Delta\eta/\eta_0)A^{(b)}_{1,0}, \tag{24}$$

for a system with an interface, where the dimensionless function ς is expected to depend on the viscosities solely *via* the dimensionless ratio $\varepsilon = \Delta\eta/\eta_0$. Since in the limit $\varepsilon \to 0$, which renders the homogeneous bulk fluid case, one has $A_{1,0} \to A^{(b)}_{1,0}$, the function ς must obey the constraint $\varsigma(\varepsilon \to 0) = 1$.

By combining eqn (9), (12), (14) and (21)–(24), we obtain

$$U_x = \frac{1}{\sqrt{3\pi}}\frac{\varsigma\left(\frac{\Delta\eta}{\eta_0}\right)}{1-\frac{3}{32}\left(\frac{\Delta\eta}{\eta_0}\right)^2}\cos(\delta)V_0 + \mathscr{O}\left(\left(\frac{\Delta\eta}{\eta_0}\right)^3\right), \tag{25a}$$

$$\Omega_z = \frac{3}{8}\frac{1}{R}\frac{\Delta\eta}{\eta_0}U_x + \mathscr{O}\left(\left(\frac{\Delta\eta}{\eta_0}\right)^3\right), \tag{25b}$$

where

$$V_0 := \frac{\mathscr{L}A^{(b)}_{1,0}}{\beta\eta_0 R} = \kappa\frac{\mathscr{L}Q}{\beta\eta_0 D_0} \tag{26}$$

renders the characteristic translational and angular velocity scales $|V_0|$ and $\Omega_0 = |V_0|/R$, respectively. V_0 is independent of the particle radius R as well as of the value of the viscosity η_0 because, under the assumption of the Stokes–Einstein relation, $\beta\eta_0 D_0$ depends only on the radius R_m of the product molecules. This implies that the translational velocity is independent of the radius R of the particle while the angular velocity is proportional to $1/R$ (up to eventual additional dependencies on R arising from ς).

Eqn (25) shows that both the translational and the angular velocity are proportional to $\cos(\delta)$. Therefore both vanish for $\delta = \pi/2$ which matches with the fact that in this case the particle is in fully upright orientation and thus cannot propel laterally. Moreover, both U_x and Ω_z change sign when the director $\mathbf{p}$ (Fig. 2(a)) changes from pointing mainly to the right to pointing mainly to the left (Fig. 2(b)). On the other hand, the sign of the ratio U_x/Ω_z, which, according to the discussion of Fig. 2(b) in the main text, decides on the sustainability of the motile state, is independent of δ but is determined by the sign of $\Delta\eta$. This is in agreement with the symmetry exhibited by the diagram shown in Fig. 2(b). In the limit of a vanishing viscosity contrast $\Delta\eta/\eta_0$, U_x approaches the constant value $V_0\cos(\delta)/\sqrt{3\pi}$. (This corresponds to the motion in a homogeneous bulk fluid under the constraint of moving along a plane at an angle δ with respect to the orientation of the director position.) Thus, for small values of $\Delta\eta$, $U_x(\Delta\eta)$ does not vary much, while, as expected, the angular velocity vanishes linearly $\propto\Delta\eta/\eta_0$. In the limiting case $\Delta\eta \to 0$ translation and rotation are decoupled and the particle translates without any rotation because there is no viscosity contrast. In such a case the net effect of the interface is to keep the particle center bound to the plane of the interface.

While the diagram in Fig. 2 is entirely determined by the ratio U_x/Ω_z, which is independent of ς, the magnitudes of both U_x and Ω_z do depend on it *via* the amplitude $A_{1,0}$ (eqn (25) and (26)). Since determining the exact form of $\varsigma(\varepsilon)$ is clearly analytically intractable, one can try to analyze its behavior for $\varepsilon \ll 1$. One option is to employ a perturbation series in terms of the

small parameter ε in order to calculate the distribution of solute for $\varepsilon \ll 1$, starting from the known solution $\rho_0(\mathbf{r})$ for $\varepsilon = 0$ (*i.e.*, for a homogeneous bulk fluid without the interface), from which one can estimate $A_{1,0}$ and implicitly $\zeta(\varepsilon)$. (Note that $\rho_0(\mathbf{r})$ varies spatially due to the solute sources located at the surface of the particle and the solute sink at infinity.) We denote by $\tilde{\rho}(\mathbf{r}) := \rho(\mathbf{r}) - \rho_0(\mathbf{r})$ and $\tilde{D}(\mathbf{r}) := D(\mathbf{r}) - D_0$ the deviations (first order in ε) of the number density distribution and of the diffusion coefficient from their corresponding values $\rho_0(\mathbf{r})$ and D_0 (spatially constant) in a homogeneous medium. (Note that by assuming the Stokes–Einstein relation between the diffusion coefficient and the viscosity $\tilde{D}(\mathbf{r})$ is a known function determined by D_0, ε, and the known variation of the viscosity across the interface (eqn (1)).) From eqn (16) and (17) one obtains that $\tilde{\rho}$ is the solution of the differential equation

$$\nabla\cdot(\tilde{D}\nabla\rho_0 + D_0\nabla\tilde{\rho}) = 0, \tag{27}$$

subject to the boundary conditions

$$\lim_{r\to\infty} \tilde{\rho} = 0, \left(\tilde{D}\nabla\rho_0 + D_0\nabla\tilde{\rho}\right)\cdot\mathbf{n}\big|_{r=R} = 0. \tag{28}$$

We have been unable to find an analytical solution of eqn (27) and (28) for a general orientation of the (small) cap. Therefore we cannot make any further rigorous statements. Instead, we only formulate expectations concerning the behavior of $\zeta(\varepsilon)$. For example, considering the case in which the catalytic cap is in the upper fluid region ($y > 0$), $\varepsilon > 0$ (*i.e.*, enhanced [reduced] viscosity in the upper [lower] fluid) leads to a reduction [increase] of the diffusion coefficient in the upper [lower] fluid. Compared with the homogeneous fluid ($\varepsilon = 0$), intuitively this should lead to a relative accumulation of product molecules near the catalytic pole (located in the upper fluid) and to a relative depletion near the inert antipole (which is located in the lower fluid). For $\varepsilon < 0$ the behavior is reversed. Since (as discussed after eqn (22)) the coefficient $A_{1,0}$ can be viewed as a measure of the difference between the densities at the catalytic pole and at the antipole, the reasoning above suggests that, upon deviating from the homogeneous state (with $A_{1,0}^{(b)}$), $A_{1,0}$ varies oppositely if the viscosity of fluid "1" relative to that of fluid "2" increases or decreases, respectively. Therefore, to first order in ε the function $\zeta(\varepsilon)$ is expected to vary as $\zeta(\varepsilon \to 0) = 1 + \text{const}\cdot\varepsilon + \mathcal{O}(\varepsilon^2)$.

4.3 Persistence length and effective diffusion coefficient for a chemically active Janus colloid at fluid interfaces

The motion of active particles is characterized by distinct regimes occurring at different timescales. At short timescales the active motion amounts to a ballistic trajectory whereas at larger timescales the behavior is diffusive. A key parameter, which characterizes the motion of active particles, is the persistence length (which can be defined as below irrespective of whether the active particle is trapped at an interface or moving in a bulk fluid)

$$\lambda = \bar{v}\tau. \tag{29}$$

This is the typical distance a Janus particle, moving at an instantaneous velocity $\bar{v}$, covers before thermal fluctuations will eventually change its direction. The time τ is determined by the rotational diffusion of the particle (see ref. 40). In the present case of the active particle being trapped at the interface there are two types of rotations. First, there are rotations of the catalytic cap orientation, *i.e.*, of $\mathbf{p}$ around the interface normal, with a characteristic time $\tau_\parallel$. These rotations lead $\mathbf{p}$ out of the initial plane of motion spanned by $\mathbf{p}$ and the interface normal. This clearly changes the direction of motion. Second, there are fluctuations of $\mathbf{p}$ within the plane of motion with the normal of the plane of motion acting as the rotation axis. Small fluctuations of this kind do not change the direction of motion because $\mathbf{p}$ remains within the initial plane of motion. However, large fluctuations can rotate $\mathbf{p}$, within the plane of motion, from a predominantly forward direction to a predominantly backward direction so that the particle runs backwards along the same straight line. This flipping of directions is associated with a timescale $\tau_\perp$. The minimum of these two timescales sets the rotational diffusion time $\tau_i = \min(\tau_\perp,\tau_\parallel)$ for an active particle trapped at an interface.

In the absence of thermal fluctuations the distribution function of the orientation of the axis $\mathbf{p}$ of the particle is peaked at the steady state value. Thermal fluctuations promote a broadening of the distribution. Both cases of rotations translate into fluctuations of the value of the instantaneous velocity of the particle. Accordingly, the typical velocity $\bar{v}_i$ of an active particle trapped at an interface is defined as the mean velocity of the Janus particle obtained as a weighted integral over all those possible configurations which give rise to a velocity with the same prescribed sign.‡‡ Before entering into further technical details concerning the definition of $\bar{v}_i$, it is convenient to focus on one of the eight cases shown in Fig. 2(b), namely the case of a Janus particle characterized by $V_0 < 0$ (see eqn (26) for repulsive solute–particle interactions so that $\mathscr{L} < 0$) and with the catalytic cap in the upper phase with $\delta < \pi/2$ (so that $\chi = \delta > 0$). For $\Delta\eta > 0$, and within the linear regime $\varepsilon \ll 1$, eqn (25) renders, in this case, $U_x < 0$ and $\Omega_z < 0$. This is the situation illustrated in the right part of the top right quadrant of Fig. 2(b). The other cases can be discussed along the same line. Accordingly, we define $\bar{v}_i$ as

$$\bar{v}_i = \left|\int_{\delta_m}^{\pi/2} \mathscr{S}(\delta)U_x(\delta)\mathrm{d}\delta\right|, \tag{30}$$

where $\mathscr{P}(\delta)$ is the steady state probability distribution to find a Janus particle with its axis forming an angle $\delta \in (\delta_m,\pi/2)$ with the plane of the interface;§§ δ_m is the value of δ for which the catalytic cap would touch the interface (see Fig. 1(b)).

‡‡ Since in the present case the system does not undergo any spontaneous symmetry breaking, the velocity obtained by averaging over all possible configurations, rather than only over those with a prescribed sign of the velocity, is zero.
§§ The mean velocity $\bar{v}_i$ for the same particle moving in the positive direction would be $\bar{v}_i = \int_{\pi/2}^{\pi-\delta_m} \mathscr{L}(\delta)U_x(\delta)\mathrm{d}\delta$; see the left part of the top right quadrant of Fig. 2(b). Here $\mathscr{P}$ is the distribution of the angle $\delta \in (\pi/2,\pi - \delta_m)$.

In thermal equilibrium, $\mathscr{P}(\delta) = \mathscr{P}_{eq}(\delta)$ depends only on the effective interactions between the catalytic cap and the interface. For example, in the absence of such interactions one has $\mathscr{P}_{eq}(\delta) = (\pi/2 - \delta_m)^{-1}$. In contrast, in the presence of an effective attraction we expect that $\mathscr{P}_{eq}(\delta)$ exhibits a peak closer to the interface (*i.e.*, close to $\delta = 0$) while the opposite holds in the case of an effective repulsion for which one expects $\mathscr{P}_{eq}(\delta)$ to be peaked at $\delta = \pi/2$. When particles are active, an additional torque arises due to the catalytic activity, hence modifying the shape of $\mathscr{P}(\delta)$. In order to estimate $\mathscr{P}(\delta)$ for active particles, we assume that $\mathscr{P}(\delta)$ factorizes as $\mathscr{P}(\delta) = \mathscr{P}_{eq}(\delta)\mathscr{P}_{neq}(\delta)$ into an equilibrium part $\mathscr{P}_{eq}(\delta)$ (as discussed above) and a modulation $\mathscr{P}_{neq}(\delta)$ due to the particle activity. As far as $\mathscr{P}_{neq}(\delta)$ is concerned, we assume that, although the system is out of thermal equilibrium, we can express it as a Boltzmann weight $\mathscr{P}_{neq}(\delta) \propto e^{-\beta\Phi(\delta)}$ of an effective potential $\Phi(\delta)$ accounting for the torque arising due to the particle activity. (This assumption is based on the fact that $\mathscr{P}_{neq}(\delta)$ is the steady-state solution of a one-dimensional (with respect to δ) advection–diffusion equation with zero current. It is known that for such systems the steady-state solution has the form of a Boltzmann weight.[41]) Since within the present model there are no effective interactions with the interface, $\mathscr{P}_{eq}(\delta)$ is a constant which can be absorbed into the normalization:

$$\mathscr{P}(\delta) := \mathscr{P}_{eq}(\delta)\mathscr{P}_{neq}(\delta) = \frac{e^{-\beta\Phi(\delta)}}{Z} \tag{31}$$

where $Z = \int_{\delta_m}^{\pi/2} e^{-\beta\Phi(\delta)} d\delta$ ensures that $\int_{\delta_m}^{\pi/2} \mathscr{P}(\delta) d\delta = 1$.

An estimate of the potential Φ can be obtained as follows. According to eqn (44), in our model a Janus particle, trapped at the interface and spinning with angular velocity Ω_z around an axis which is contained in the plane of the interface and passes through the center of the particle, experiences a torque $L_z = -8\pi\eta_0 R^3 \Omega_z$. Therefore, in order to maintain the angular velocity $\Omega_z(\delta)$ of the particle an external torque equal to $-L_z$ must be applied to the particle. Accordingly, for the Janus particle translating with $U_x(\delta)$ while simultaneously rotating with $\Omega_z(\delta)$, we introduce an effective torque

$$L(\delta) = 8\pi\eta_0\Omega_z(\delta)R^3 \tag{32}$$

analogous to the external one which would have accounted for the same angular velocity, and define, *via* $L(\delta) = -d\Phi(\delta)/d\delta$, the effective potential $\Phi(\delta)$ as

$$\beta\Phi(\delta) := -\beta\int_{\delta_m}^{\delta} L(\delta')d\delta' \overset{(25),(26)}{=} \Pi[\sin(\delta_m) - \sin(\delta)]. \tag{33}$$

In this equation one has $\Pi = \sqrt{3\pi}\beta V_0 R^2 \Delta\eta$, the reference potential is set to $\Phi(\delta_m) = 0$, and we have accounted for the fact that here we discuss only the case in which $\delta_m \le \delta \le \pi/2$ (each of the other three quadrants can be analyzed following the same line of reasoning).

The sign of Π is determined by the sign of V_0 and $\Delta\eta$. As we noted above, here we focus on the case in which $V_0 < 0$ (*i.e.*, there is a repulsive interaction between the Janus particle and the product molecules of the catalysis) so that $\Pi = -\sqrt{3\pi}\beta|V_0|R^2\Delta\eta = -1/(2\sqrt{3\pi})(\Delta\eta/\eta_0)\mathrm{Pe}_0$, where $\mathrm{Pe}_0 = |V_0|R/D_P > 0$ is the Péclet number of a Janus particle in a homogeneous fluid of viscosity η_0 and $D_P = k_B T/(6\pi\eta_0 R)$ is the diffusion constant of the Janus particle defined *via* the Stokes–Einstein relation. The above expression for Π shows that, for $\Delta\eta > 0$ and a Janus particle characterized by $V_0 < 0$, Π is negative. In this case one has $\Phi(\delta > \delta_m) > 0$ (eqn (33)) and thus $\Phi(\delta)$ attains its minimum at $\delta = \delta_m$. This means that the action of the effective torque is consistent with $\Omega_z < 0$ (see eqn (25b)) which "drives" the particle towards its steady-state orientation δ_m, as discussed in Fig. 2(b) (right part of the top right quadrant). Accordingly, in the right part of the top right quadrant, corresponding to $\Delta\eta > 0$ and to the director pointing into the upper fluid, consistent with $\delta_m \le \delta < \pi/2$ and thus $\chi = \min(\delta, \pi - \delta) > 0$, repulsive interactions (orange arrows) ensure a sustained motility state by providing a torque which tilts the director towards the interface, *i.e.*, which in the present case leads to a decrease of δ towards δ_m. As one can read off from eqn (33), the characteristics of the Janus particle (see eqn (26)) and of the fluid phases are all encoded in Π. Therefore the above conclusions can be extended directly to the case of attractive interactions between the Janus particle and the product molecules of the catalytic reaction by changing the sign of V_0, and hence of Π. Therefore, in the case of attractive interactions (*i.e.*, $V_0 > 0$) and with the cap oriented such that $\delta_m \le \delta < \pi/2$ and $\chi = \delta > 0$, Π is negative for $\Delta\eta < 0$ and thus $\Phi(\delta > \delta_m) > 0$ (in agreement with the situation illustrated in the left part of the top left quadrant of Fig. 2(b) for which $U_x > 0$ and $\Omega_z < 0$). Therefore, if particles have the catalytic cap in the upper phase, for which $\sin(\delta) > 0$, the states with small values of $\sin(\delta)$, *i.e.*, with the catalytic patch being closer to the interface and thus promoting the motile state, are favored if $\Pi < 0$. Similarly, if the catalytic cap of the particle is in the lower phase, where $\sin(\delta) < 0$, large values of $\sin(\delta)$, *i.e.*, the catalytic patch being closer to the interface and thus promoting the motile state, are favored if $\Pi > 0$.

Concerning the persistence length $\lambda_i = \bar{v}_i\tau_i$ of an active particle trapped at an interface (eqn (29) and (30)) one would like to understand its relation to the persistence length $\lambda_b = \bar{v}_b\tau_b$ of a similar active particle moving freely in a homogeneous bulk fluid. To this end, we proceed by assuming that the characteristic time τ_i for the loss of orientation of a Janus particle, trapped at and moving along an interface between two fluids characterized by a (not too large) viscosity contrast $\Delta\eta \neq 0$, is similar to the corresponding characteristic rotational diffusion time τ_b for the loss of orientation in a homogeneous bulk fluid of viscosity η_0.¶¶ However, since one of the three possible independent rotations of a rigid body would affect the directionality for the particle trapped at the interface only if it is associated with a large fluctuation which would flip the director **p** with respect to the interface normal (see the discussion of $\tau_\perp$ after eqn (29)), it is a reasonable to expect that $\tau_i > \tau_b$. Furthermore, the argument concerning the weak influence of

¶¶ It is particularly difficult to determine τ_i because it depends on the details of the effective interaction between the Janus particle and the interface and it involves the dynamics of the moving three-phase contact line.

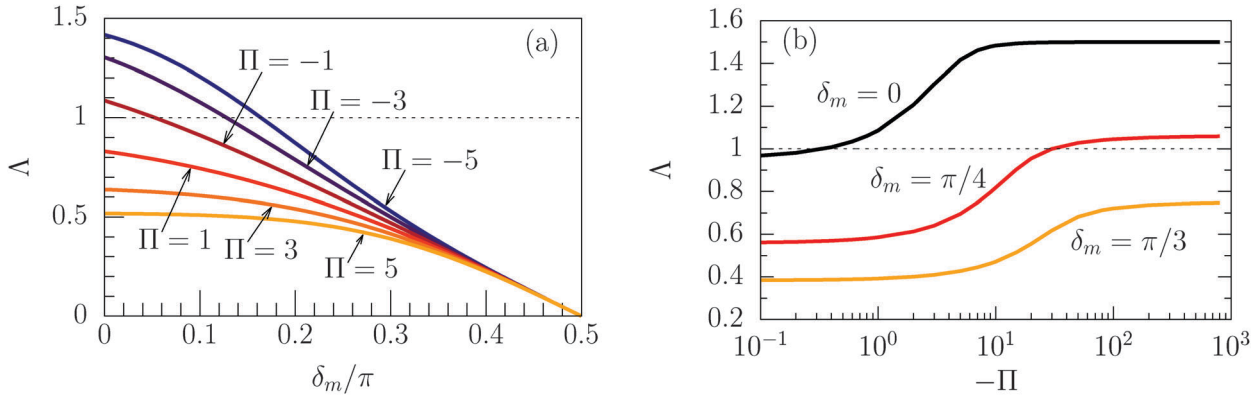

Fig. 3 (a) Approximate expression for the ratio $\Lambda = \lambda_i/\lambda_b$ (eqn (34) with $\nu_0 = 3/2$) of the persistence length of a Janus particle at the interface (λ_i, catalytic cap in the upper phase) and in the bulk (λ_b) as a function of δ_m for various values of $\Pi = \sqrt{3\pi}\beta V_0 R^2 \Delta\eta$. The angle δ_m is the opening angle under which the catalytic cap is seen from the center of the particle when the cap touches the interface (Fig. 1(b)) and thus measures its size. (b) Approximate expression for Λ as a function of $-\Pi > 0$ for $\delta_m = 0$, $\pi/4$, and $\pi/3$. Although the value $\delta_m = 0$ is unphysical, because in this case the catalytic cap reduces to a point, the corresponding curve represents the limiting case for which Λ attains its maximal values.

the rotations associated with $\tau_\perp$ suggests $\tau_i = \nu_0\tau_b$ with $\nu_0 \simeq 3/2$ as a good ansatz for the relationship between the two characteristic timescales. Furthermore, we note that eqn (25b) has the form of a projection onto the x-axis (due to the factor $\cos(\delta)$) of a velocity (the factor multiplying $\cos(\delta)$) oriented along the director $\mathbf{p}$. Thus in the limit $\Delta\eta \to 0$ the latter factor can be identified with the velocity $\bar{v}_b$ of the active particle moving in a homogeneous bulk fluid of viscosity η_0. With $\varsigma(\varepsilon \to 0) = 1$ this renders $\bar{v}_b = \frac{1}{\sqrt{3\pi}}|V_0|$.

From eqn (30) and (31), after disregarding corrections to U_x of order $\varepsilon = \frac{\Delta\eta}{\eta_0}$ (eqn (25a)), one obtains

$$\Lambda := \frac{\lambda_i}{\lambda_b} \simeq \frac{\tau_i}{\tau_b}\frac{\bar{v}_i}{\bar{v}_b} \simeq \nu_0 \int_{\delta_m}^{\pi/2} \frac{e^{-\beta\Phi(\delta)}}{Z}\cos(\delta)\mathrm{d}\delta \qquad (34)$$

By inserting $Z = \int_{\delta_m}^{\pi/2} e^{-\beta\Phi(\delta)}\mathrm{d}\delta$ and eqn (33) into eqn (34), the dependencies of Λ on δ_m and on Π can be calculated. For the choice $\nu_0 = 3/2$ these are shown in Fig. 3(a) and (b), respectively. (We recall that we have focused on the case of the catalytic cap exposed to the upper phase.) As shown in Fig. 3, for sufficiently negative values of Π the persistence length of a Janus particle moving at a liquid–fluid interface may be larger than the one in the corresponding bulk case, *i.e.*, $\Lambda > 1$. According to the discussion in the previous paragraphs, the case of $\Pi > 0$ with the catalytic cap exposed to the upper phase corresponds to either $\Delta\eta > 0$ and repulsive interactions or $\Delta\eta > 0$ and attractive interactions, *i.e.*, the cases for which sustained motility emerges (see Fig. 2(b)). On the other hand, we have noted that for a given type of interaction (*i.e.*, a given sign of V_0) and a given viscosity contrast $\Delta\eta$, the amplitude Π of the potential Φ changes sign if the catalytic cap is exposed to the lower phase, *i.e.*, for $\delta > \pi$, relative to the case of the catalytic cap being exposed to the upper phase. Therefore, these corresponding dependencies on δ_m and on Π are given by the curves in Fig. 3(a) and (b) but with the opposite sign of Π and with $\delta_m \to -\delta_m$. Consequently, one infers that in this case one has $\Lambda > 1$ for sufficiently large positive values of Π. Thus also in the case that the cap is immersed in the lower phase the persistence length at the interface may be enhanced relative to the bulk one for those states in which sustained motility emerges. In summary, this implies that in all cases of sustained motility (*i.e.*, the system corresponds to any of the cases shown in Fig. 2(b)) the particle trapped at the interface exhibits an enhanced persistence length for sufficiently large values of $|\Pi|$.

Fig. 3(b) shows the dependency of Λ on Π for the case in which the catalytic cap is exposed to the upper phase. Interestingly, Λ saturates at negative values of Π with large $|\Pi|$. The saturation occurs at larger values of $|\Pi|$ upon increasing δ_m. Concerning the magnitude of Π at which Λ starts to saturate, we recall that $|\Pi| = \frac{1}{2\sqrt{3\pi}}\frac{\Delta\eta}{\eta_0}\mathrm{Pe}_0$. Therefore, for $\frac{\Delta\eta}{\eta_0} \to 0$ the onset of saturation at $|\Pi| \approx 5$ requires, even for very small caps, *i.e.*, $\delta_m \to 0$, Péclet numbers $\mathrm{Pe}_0 \simeq 30 \times (\Delta\eta/\eta_0)^{-1}$ much larger than the typical values $\mathrm{Pe}_0 \simeq 10$ for Janus particles in a homogeneous bulk fluid. If, however, the viscosity contrast is high, the required corresponding Pe_0 numbers are significantly smaller. For example, for the water–air interface the viscosity of air is negligible so that $\Delta\eta = -2\eta_0$ which implies $|\Pi| \simeq \frac{1}{3}\mathrm{Pe}_0$. In such a situation, as well as for other liquid–fluid interfaces characterized by high viscosity contrasts, large values of $|\Pi|$ are encountered already for typical values of Pe_0 and the persistence length at the interface may be enhanced relative to its bulk value, *i.e.*, $\Lambda > 1$. As shown in Fig. 3, this effect is particularly pronounced for small catalytic caps (*i.e.*, δ_m small).

While the persistence length λ characterizes the active motion of a particle at timescales shorter than the characteristic rotational diffusion time τ, at timescales much larger than τ the motion of the particle crosses over to diffusion with an effective diffusion constant:[40]

$$D_{\mathrm{eff}} = D_{\mathrm{tr}} + \frac{\lambda^2}{\tau} := D_{\mathrm{tr}} + \delta D, \qquad (35)$$

where D_{tr} is the translational diffusion constant of the particle in the absence of activity and $\delta D = \lambda^2/\tau$ is the activity-induced enhancement of the diffusion constant. Eqn (35) allows us to compare the enhancement $\delta D^{(i)}$ for the Janus particle trapped at, and moving along, the interface to the one, $\delta D^{(b)}$, which holds for the same active Janus particle moving in a bulk fluid:

$$\frac{\delta D^{(i)}}{\delta D^{(b)}} = \left(\frac{\lambda_i}{\lambda_b}\right)^2 \frac{\tau_b}{\tau_i} \simeq \frac{1}{\nu_0} \Lambda^2. \tag{36}$$

Therefore, according to the values of Λ shown in Fig. 3, for $\nu_0 = 3/2$ the enhancement of the diffusion constant due to the activity of a Janus particle trapped at a liquid–fluid interface can be up to 1.5 times larger than the enhancement observed in a homogeneous bulk fluid. Finally, we note that for a particle trapped at the interface the activity induced contribution $\delta D^{(i)}$ can become much larger than the passive translational diffusion constant D_P in bulk fluid if $(\bar{v}_i^2 \tau_i^2)/(\tau_i D_P) \gg 1$ (see the definition of $\delta D^{(i)}$ above and eqn (29)). By using $\bar{v}_i = \Lambda \bar{v}_b/\nu_0$ (eqn (34)), $\bar{v}_b = V_0/\sqrt{3\pi}$, $Pe_0 = |V_0|R/D_P$, and $\tau_i/\tau_b = \nu_0$, and by taking $\tau_b = 1/D_P^{(rot)}$, where $D_P^{(rot)} = 4D_P/(3R^2)$ is the rotational diffusion constant of the particle in a homogeneous bulk fluid,[40] for $\nu_0 = 3/2$ and by using eqn (34)–(36) the condition $\delta D^{(i)}/D_P \gg 1$ translates into the condition $Pe_0 \gg 4.3/\Lambda$ for the Péclet number of the particle.

5 Summary and conclusions

We have studied the behavior of a chemically active Janus particle trapped at a liquid–fluid interface, under the assumptions that the activity of the particle does not affect the surface tension of the interface and that the interface can be assumed to be flat. If particles are moving in such a set-up (Fig. 1), a coupling between rotation and translation arises due to the viscosity contrast $\Delta\eta$ between the two adjacent fluids. Assuming that the particles are axisymmetric, and that both fluid phases are homogeneous and isotropic, the motile state of the particles is characterized by their linear velocity U_x in the plane of the interface and their angular velocity Ω_z about an axis perpendicular to the plane of motion spanned by the interface normal and the velocity.

In Section 3 we have determined the linear and angular velocity U_x and Ω_z, respectively, by using the Lorentz reciprocal theorem.[35] Therein the stress-free interface is accounted for by imposing the corresponding boundary conditions on the fluid flow in both phases and the fluids are taken to be quiescent far away from the particle. The result in eqn (6) is valid for an arbitrary viscosity contrast $\Delta\eta$, including the limit of vanishing values of $\Delta\eta$ as well as the case that one of the two phases has a vanishing viscosity.

Determining U_x and Ω_z *via* the reciprocal theorem requires to solve two independent auxiliary problems involving translation and rotation of a particle trapped at a liquid–fluid interface. In order to be able to obtain analytical solutions, we have considered neutrally buoyant particles exhibiting a contact angle of $\pi/2$ with the planar interface. Under these assumptions it is possible to exploit the available analytical solution for the stress exerted on the fluid by a particle which is translating without rotation.[28] The case of a particle rotating at the interface is more challenging because it requires to determine the fluid flow close to the three-phase contact line formed as the intersection of the interface and the particle surface. In order to circumvent the issue of the motion of the three-phase contact line and in order to gain analytical insight into the problem, we have assumed that the fluid slips along the particle only in a small region close to the three-phase contact line. Accordingly, we can consider the fluid flow on each part of the surface of the particle to be *de facto* equal to the one which a particle experiences in a corresponding homogeneous bulk fluid under no-slip conditions on its surface (eqn (11)). The general expressions for U_x and Ω_z (eqn (14a) and (b)) show that, for $\Delta\eta \neq 0$, Ω_z is nonzero. Therefore the motility of the particle along the interface is strongly affected by the change in the orientation of the axis of the particle relative to the interface normal. Accordingly, the velocity of the particle along the interface can be either enhanced or reduced.

In Section 4A we have established a diagram (Fig. 2) describing the situations for which Ω_z promotes orientations of the Janus particle axis to be parallel to the interface, hence enforcing the motile state of the particle. In particular, for repulsive interactions between the particle and the self-generated solute (*e.g.*, for catalytic platinum caps on polystyrene particles suspended in water–peroxide solutions‖‖) we have found that the motile state is fostered if the catalytic cap is immersed into the more viscous phase, while the opposite conclusion holds for an attractive interaction. Therefore, by tuning the viscosity contrast $\Delta\eta$, one can control the motility of Janus particles trapped at liquid–fluid interfaces.

In Section 4B these general considerations have been extended further by specifying model particles which allow one to analyze the density profiles of the reaction product. The expansion of these profiles in terms of spherical harmonics shows that only the amplitude $A_{1,0}$ of the largest wavelength mode affects U_x and Ω_z (see Appendix B). Accordingly, for the model considered here, different systems characterized by diverse physical properties (such as the viscosity contrast $\Delta\eta$, the catalytic reaction, or the interaction between the reaction product and the particle) but exhibiting the same value of $A_{1,0}$ lead to the same values of U_x and Ω_z (see eqn (25a) and (25b)). In particular we have found that both U_x and Ω_z are proportional to the velocity scale V_0 (eqn (26)) which depends linearly on the prefactor $\mathscr{L}$ (see eqn (15)), the reaction rate Q per area, the inverse mean viscosity η_0 and the inverse diffusivity D_0 of the reaction product. The angular velocity experienced by the particle of radius R is proportional to V_0/R and to the viscosity contrast $\Delta\eta$.

‖‖ In this case the repulsive character of interaction is inferred from the experimentally observed motion away from the platinum cap and under the assumption that the mechanism of motion is self-diffusiophoresis and that only the oxygen production and the corresponding surface gradients of oxygen are relevant.

If the angular velocity promotes the alignment of the axis of the particle with the interface, the persistence length of the particle increases. In order to quantify this effect, in Section 4.3 we have proposed a factorization of the probability distribution (eqn (31)) for the orientation of the axis of the particle into an equilibrium and into a non-equilibrium distribution induced by the angular velocity and we have constructed an effective potential Φ (eqn (33)) describing the latter. The strength $|\Pi|$ (eqn (33)) of this potential is proportional to the bulk Péclet number of the particle, which is of the order of 10, and therefore may lead to an increase of the persistence length of a trapped active particle relative to its value in the bulk fluid. Fig. 3(b) shows that this enhancement increases with $|\Pi|$ as well as upon decreasing the size of the catalytic cap (which allows for smaller values of δ_m (see Fig. 1(b) and 3(a)). At long timescales the motion of active Janus particles is characterized by an effective diffusion coefficient (see eqn (35)). Concerning this regime our results predict that $\Delta\eta$ as well as Π control the enhancement of the effective diffusion coefficient. In particular, by using eqn (36) and the data in Fig. 3, we have found that the presence of the interface can almost double the activity induced enhancement of the diffusion coefficient compared with the one in a homogeneous bulk fluid.

In sum we have obtained the following main results:

- Within a minimalistic model of active Janus particles trapped at a liquid–fluid interface, we have characterized their dynamics and have shown that their motility is strongly affected by the angular velocity induced on the particle due to the viscosity contrast $\Delta\eta$ between the adjacent fluids.
- We have shown that the rotation–translation coupling induced by $\Delta\eta$ can affect experimentally observable quantities such as the persistence length and the effective diffusion coefficient of active Janus particles trapped at liquid–fluid interfaces. In particular, the behavior described by our model is in agreement with recently reported, corresponding experimental observations of increased persistence lengths for chemically active Janus particles at water–air interfaces,[22] and it sheds light on the proposition of an alternative explanation for the observed phenomenon.
- Since the viscosity contrast $\Delta\eta$ can control the performance of active particles moving at liquid–fluid interfaces, we suggest that it can be relevant also for the onset of instabilities of thin films covered by active particles.[42]

Finally, we mention a few interesting extensions of the present study. Relaxing some of the simplifying assumptions employed here might shed light on alternative means to control active particle motility at liquid–fluid interfaces. In this respect we recall that we have assumed that the contact angle of the particle with the interface is $\pi/2$, and that pinning of the three-phase contact line is absent. Concerning the contact angle, we expect particles with a contact angle unequal $\pi/2$ to experience extra torques due to the offset of their center of mass from the plane of the interface. A similar scenario has been reported for particles which are pulled, without rotating, under the action of suitably distributed external forces and torques.[28] On the other hand, pinning of the three-phase contact line might affect the effective rotational diffusion and, possibly, suppress it, as shown recently for an equilibrium system.[43] Therefore we expect that for active Janus particles trapped at liquid–fluid interfaces the pinning of the three-phase contact line can enhance the persistence length, and therefore the effective diffusion, as argued in ref. 22, too.

Appendix

A Forces and torques

Here we present the steps of the derivations leading to eqn (9) and (12). In order to simplify the calculations, here it is convenient to translate the origin O of the unprimed coordinate system (fixed in space, see Fig. 1(b)) to the center C of the moving particle and to use spherical coordinates (r, θ, ϕ), which are defined as usual: $x = r\sin(\theta)\cos(\phi)$, $y = r\sin(\theta)\sin(\phi)$, and $z = r\cos(\theta)$. (Note that these are defined in the unprimed coordinate system which, although exhibiting here the same origin as the primed (co-moving) one, has different orientations of the axes as compared with the primed one. The unprimed coordinate system offers a less cumbersome parametrization of the location of the interface as compared with the primed coordinate system.) We start with deriving eqn (9).

By using that for a translation (only) with velocity $\hat{\mathbf{U}} = \hat{U}_x\mathbf{e}_x$ one has[28]

$$\mathbf{n}\cdot\hat{\boldsymbol{\sigma}}|_{\Sigma_p} = -\frac{3}{2R}\eta(\mathbf{r}_p)\hat{\mathbf{U}} \tag{37}$$

on the surface Σ_p of the particle. By noting that

$$\hat{F}_x = \int_{\Sigma_p}(\mathbf{n}\cdot\hat{\boldsymbol{\sigma}})_x \mathrm{d}S \tag{38}$$

is the x component of the integral over the surface of the normal pressure tensor as given by the above expression, using eqn (1), and assuming a sharp interface ($\xi \to 0$ so that $\eta(\mathbf{r}_p) = \eta(\phi)$ with $\eta(\phi) = \eta_1$ for $0 < \phi < \pi$, *i.e.*, $y > 0$, while $\eta(\phi) = \eta_2$ for $\pi < \phi < 2\pi$, *i.e.*, $y < 0$) one obtains

$$F_x = -\frac{3}{2R}\hat{U}_x R^2 \int_0^{\pi}\mathrm{d}\theta\sin(\theta)\int_0^{2\pi}\mathrm{d}\phi\eta(\phi) = -6\pi\eta_0 R\hat{U}_x, \tag{39}$$

which agrees with eqn (9a). The torque is defined as

$$\begin{aligned}\mathbf{L} &= \int_{\Sigma_p}(\mathbf{r}_p - \mathbf{r}_C)\times\hat{\boldsymbol{\sigma}}\cdot\mathbf{n}\mathrm{d}S = R\int_{\Sigma_p}\mathbf{n}\times\hat{\boldsymbol{\sigma}}\cdot\mathbf{n}\mathrm{d}S \\ &= -\frac{3}{2}\int_{\Sigma_p}\eta(\mathbf{r})\mathbf{n}\times\hat{\mathbf{U}}\mathrm{d}S,\end{aligned} \tag{40}$$

where we have used $\mathbf{r}_p - \mathbf{r}_C = R\mathbf{n}$ (see Fig. 1). With the above choice of the coordinate system the torque is along the z-direction. Since $(\mathbf{n}\times\hat{\mathbf{U}})_z = n_x\hat{U}_y - n_y\hat{U}_x$ and $\hat{U}_y = 0$ (due to the choice of the dual problem "1"), with $n_y = \sin(\theta)\sin(\phi)$ one obtains

$$L_z = \frac{3}{2}R^2\hat{U}_x\int_0^{\pi}\mathrm{d}\theta\sin^2(\theta)\int_0^{2\pi}\mathrm{d}\phi\sin(\phi)\eta(\phi) = \frac{3}{2}\pi R^2\Delta\eta\hat{U}_x, \tag{41}$$

which agrees with eqn (9b).

Concerning the derivation of eqn (12) we start from the relation (compare eqn (11) with $\hat{\mathbf{\Omega}} = \Omega_z \mathbf{e}_z$)

$$\mathbf{n} \cdot \hat{\boldsymbol{\sigma}}|_{\Sigma_p} = -3\eta(\mathbf{r}_\mathrm{p})\hat{\mathbf{\Omega}} \times \mathbf{n}; \tag{42}$$

we note that $\left(\hat{\mathbf{\Omega}} \times \mathbf{n}\right)_x = \hat{\Omega}_y n_z - \hat{\Omega}_z n_y$ and recall that by definition of the dual problem "2" only the component $\hat{\Omega}_z$ of the angular velocity is non-zero. Thus we obtain

$$\begin{aligned} F_x &= 3\hat{\Omega}_z R^2 \int_0^\pi \mathrm{d}\theta \sin^2(\theta) \int_0^{2\pi} \mathrm{d}\phi \sin(\phi)\eta(\phi)\mathrm{d}\phi \\ &= 3\pi R^2 \Delta\eta \hat{\Omega}_z, \end{aligned} \tag{43}$$

which agrees with eqn (12a). For the torque one has, with $\mathbf{r}_\mathrm{p} - \mathbf{r}_\mathrm{C} = R\mathbf{n}$,

$$\begin{aligned} L_z &= R\int_{\Sigma_\mathrm{p}} [\mathbf{n} \times \hat{\boldsymbol{\sigma}} \cdot \mathbf{n}]_z \mathrm{d}S = -3R\int_{\Sigma_\mathrm{p}} \eta(\mathbf{r})\left[\mathbf{n} \times (\hat{\mathbf{\Omega}} \times \mathbf{n})\right]_z \mathrm{d}S \\ &= -3R\int_{\Sigma_\mathrm{p}} \eta(\mathbf{r})\hat{\Omega}_z \sin^2(\theta)\mathrm{d}S = -3R^3\hat{\Omega}_z \int_0^\pi \mathrm{d}\theta \sin^3(\theta) \int_0^{2\pi} \mathrm{d}\phi\eta(\phi) \\ &= -8\pi\eta_0 R^3 \hat{\Omega}_z, \end{aligned} \tag{44}$$

which agrees with eqn (12b) and where the following relations have been used:

$$\hat{\mathbf{\Omega}} \times \mathbf{n} = -\begin{pmatrix} n_y\hat{\Omega}_z - n_z\hat{\Omega}_y \\ n_z\hat{\Omega}_x - n_x\hat{\Omega}_z \\ n_x\hat{\Omega}_y - n_y\hat{\Omega}_x \end{pmatrix} \tag{45}$$

and

$$\begin{aligned} \left[\mathbf{n} \times (\hat{\mathbf{\Omega}} \times \mathbf{n})\right]_z &= n_x n_y \hat{\Omega}_x + {n_x}^2 \hat{\Omega}_z + {n_y}^2 \hat{\Omega}_z + n_y n_z \hat{\Omega}_y \\ &= \hat{\Omega}_z\left({n_x}^2 + {n_y}^2\right) = \hat{\Omega}_z \sin^2(\theta). \end{aligned} \tag{46}$$

In eqn (46) we have used, according to the definition of the dual problem "2", $\hat{\Omega}_x = \hat{\Omega}_y = 0$.

B Diffusiophoretic slip

We start the derivation of eqn (21) and (22) by employing spherical coordinates (r', θ', ϕ'):

$$x' = r'\sin(\theta')\cos(\phi'), \quad y' = r'\sin(\theta')\sin(\phi'), \quad z' = r'\cos(\theta') \tag{47}$$

in the co-moving (primed) coordinate system (see Fig. 1(b)) with $\rho(\mathbf{r}_\mathrm{p}') = \rho(R, \theta', \phi')$; in the following, for reasons of shorter notations we shall not indicate explicitly the dependence on R. The density can be expressed as a series expansion in terms of the spherical harmonics $Y_{\ell m}(\theta',\phi')$:

$$\rho(\theta', \phi') = \sum_{\ell=0}^{\infty} \sum_{m=-\ell}^{m=\ell} A_{\ell,m} Y_{\ell m}(\theta', \phi'), \tag{48}$$

where[39]

$$Y_{\ell m}(\theta', \phi') = \alpha_{\ell,m} P_\ell^m(\cos\theta')\mathrm{e}^{im\phi'}, \quad i = \sqrt{-1}, \tag{49}$$

and

$$\begin{aligned} P_\ell^m(x) &= \frac{(-1)^m}{2^\ell \ell!}\left(1 - x^2\right)^{m/2} \frac{\mathrm{d}^{\ell+m}}{\mathrm{d}x^{\ell+m}}\left(x^2 - 1\right)^\ell, \quad \ell \geq 0, \\ |m| &\leq \ell \end{aligned} \tag{50}$$

is the associated Legendre polynomial of degree ℓ and order m with

$$\alpha_{\ell,m} = \sqrt{\frac{2\ell + 1}{4\pi}\frac{(\ell - m)!}{(\ell + m)!}} \tag{51}$$

as a normalization constant.

Before proceeding, we list a few relations (obtained straightforwardly from the corresponding definitions) satisfied by $Y_{\ell m}$, P_ℓ^m, and $\alpha_{\ell,m}$, which will be needed below:

$$Y_{00} = \frac{1}{\sqrt{4\pi}}, \tag{52}$$

$$P_\ell^{-m} = (-1)^m \frac{(\ell - m)!}{(\ell + m)!} P_\ell^m, \tag{53}$$

$$Y_{\ell(-m)} = (-1)^m Y_{\ell m}^*, \tag{54}$$

$$\alpha_{\ell,-m} = \frac{(\ell + m)!}{(\ell - m)!}\alpha_{\ell,m}, \tag{55}$$

$$\int_0^{2\pi} \mathrm{d}\phi' \int_0^\pi \mathrm{d}\theta' \sin\theta\, Y_{\ell' m'}^*(\theta', \phi') Y_{\ell m}(\theta', \phi') = \delta_{\ell,\ell'}\delta_{m,m'}, \tag{56}$$

$$\frac{\partial Y_{\ell m}}{\partial \phi} = im Y_{\ell m}, \tag{57}$$

and

$$\begin{aligned} \sin\theta' \frac{\partial Y_{\ell m}}{\partial \theta'} &= \ell\sqrt{\frac{(\ell + 1)^2 - m^2}{(2\ell + 1)(2\ell + 3)}} Y_{(\ell+1)m} \\ &\quad - (\ell + 1)\sqrt{\frac{\ell^2 - m^2}{(2\ell - 1)(2\ell + 1)}} Y_{(\ell-1)m} \\ &:= a_{\ell,m} Y_{(\ell+1)m} + b_{\ell,m} Y_{(\ell-1)m}, \end{aligned} \tag{58}$$

where * indicates the complex conjugate quantity.

From the definition of the phoretic slip $\mathbf{v}(\mathbf{r}'_\mathrm{P})$ (eqn (20)) one obtains

$$\eta(\mathbf{r}'_\mathrm{P})v_{\theta'} = -\frac{\mathscr{L}}{\beta R}\sum_{\ell=0}^{\infty}\sum_{m=-\ell}^{m=\ell} A_{\ell,m}\frac{\partial Y_{\ell m}(\theta', \phi')}{\partial \theta'} \tag{59}$$

and

$$\eta\left(\mathbf{r}_\mathrm{p}^{'}\right)v_{\phi'} = -\frac{\mathscr{L}}{\beta R}\frac{1}{\sin\theta'}\sum_{\ell=0}^{\infty}\sum_{m=-\ell}^{m=\ell} A_{\ell,m}\frac{\partial Y_{\ell m}(\theta', \phi')}{\partial \phi'}. \tag{60}$$

Noting that the unit vectors $\mathbf{e}_{r'}$, $\mathbf{e}_{\theta'}$, and $\mathbf{e}_{\phi'}$ are given by

$$\begin{aligned} \mathbf{e}_{r'} &= \sin\theta'\cos\phi'\,\mathbf{e}_{x'} + \sin\theta'\sin\phi'\,\mathbf{e}_{y'} + \cos\theta'\,\mathbf{e}_{z'} \\ \mathbf{e}_{\theta'} &= \cos\theta'\cos\phi'\,\mathbf{e}_{x'} + \cos\theta'\sin\phi'\,\mathbf{e}_{y'} - \sin\theta'\,\mathbf{e}_{z'} \\ \mathbf{e}_{\phi'} &= -\sin\phi'\,\mathbf{e}_{x'} + \cos\phi'\,\mathbf{e}_{y'} \end{aligned} \tag{61}$$

and using geometry (see Fig. 1(b)) one obtains

$$\begin{aligned} v_x &= v_{z'}\cos\delta = (\mathbf{v}\cdot\mathbf{e}_{z'})\cos\delta \\ &= \left(v_{\theta'}\mathbf{e}_{\theta'}\cdot\mathbf{e}_{z'} + v_{\phi'}\mathbf{e}_{\phi'}\cdot\mathbf{e}_{z'}\right)\cos\delta \overset{(61)}{=} -v_{\theta'}\sin\theta'\cos\delta; \end{aligned} \quad (62)$$

according to eqn (20) $v_{r'} = 0$. Therefore

$$\begin{aligned} C_1 &:= \frac{3}{2R}\int_{\Sigma_\mathrm{p}} \mathrm{d}S\eta\left(\mathbf{r}_\mathrm{p}^{'}\right)v_x \\ &\overset{(62)}{\underset{(59)}{=}} \frac{3}{2}\frac{\mathscr{L}\cos\delta}{\beta}\int_0^{2\pi}\mathrm{d}\phi'\int_0^{\pi}\mathrm{d}\theta'\sin\theta'\sum_{\ell=0}^{\infty}\sum_{m=-\ell}^{m=\ell}A_{\ell,m}\sin\theta'\frac{\partial Y_{\ell m}(\theta',\phi')}{\partial\theta'} \\ &\overset{(58)}{\underset{(52)}{=}} \frac{\mathscr{L}\cos\delta}{\beta}\sum_{\ell=0}^{\infty}\sum_{m=-\ell}^{m=\ell}A_{\ell,m}\Big\{a_{\ell,m}\int_0^{2\pi}\mathrm{d}\phi'\int_0^{\pi}\mathrm{d}\theta'\sin\theta' Y_{00}{}^{*}(\theta',\phi') \\ &\qquad\times Y_{(\ell+1)m}(\theta',\phi') + b_{\ell,m}\int_0^{2\pi}\mathrm{d}\phi'\int_0^{\pi}\mathrm{d}\theta'\sin\theta' Y_{00}{}^{*}(\theta',\phi') \\ &\qquad\times Y_{(\ell-1)m}(\theta',\phi')\Big\} \\ &\overset{(56)}{=} 3\sqrt{\pi}\frac{\mathscr{L}\cos\delta}{\beta}\sum_{\ell=0}^{\infty}\sum_{m=-\ell}^{m=\ell}A_{\ell,m}\left(a_{\ell,m}\delta_{0,\ell+1}\delta_{0,m} + b_{\ell,m}\delta_{0,\ell-1}\delta_{0,m}\right) \\ &= 3\sqrt{\pi}\frac{\mathscr{L}\cos\delta}{\beta}A_{1,0}b_{1,0} \overset{(58)}{=} -2\sqrt{3\pi}\frac{\mathscr{L}\cos\delta}{\beta}A_{1,0}, \end{aligned} \quad (63)$$

which agrees with eqn (21).

We now proceed with the calculation of C_2. First, we note that $\mathbf{e}_z = \mathbf{e}_{x'}$ (see Fig. 1(b)), and therefore $(\mathbf{n}\times\mathbf{v})_z := (\mathbf{n}\times\mathbf{v})\cdot\mathbf{e}_z = (\mathbf{n}\times\mathbf{v})_{x'}$, where $\mathbf{v} = \mathbf{v}(\mathbf{r}_\mathrm{p}')$. The latter but one expression is calculated as follows (note that in the primed coordinate system $\mathbf{n} = \mathbf{e}_{r'}$):

$$\begin{aligned} (\mathbf{n}\times\mathbf{v})_{x'} &= n_{y'}v_{z'} - n_{z'}v_{y'} \\ &= \left(\mathbf{e}_{r'}\cdot\mathbf{e}_{y'}\right)v_{z'} - \left(\mathbf{e}_{r'}\cdot\mathbf{e}_{z'}\right)\left[v_{\theta'}\left(\mathbf{e}_{\theta'}\cdot\mathbf{e}_{y'}\right) + v_{\phi'}\left(\mathbf{e}_{\phi'}\cdot\mathbf{e}_{y'}\right)\right] \\ &\overset{(62)}{\underset{(61)}{=}} v_{\theta'} - \cos\theta'\left(\cos\theta'\sin\phi' v_{\theta'} + \cos\phi' v_{\phi'}\right) \\ &= -\left(\sin\phi' v_{\theta'} + \cos\theta'\cos\phi' v_{\phi'}\right). \end{aligned} \quad (64)$$

Therefore C_2 takes the form (eqn (13))

$$\begin{aligned} C_2 &:= \frac{3}{R}\int_{\Sigma_\mathrm{p}}\mathrm{d}S'\eta\left(\mathbf{r}_\mathrm{p}^{'}\right)(\mathbf{n}\times\mathbf{v})_z \\ &= -3R\left(\int_0^{2\pi}\mathrm{d}\phi'\sin\phi'\int_0^{\pi}\mathrm{d}\theta'\sin\theta'\eta\left(\mathbf{r}_\mathrm{p}^{'}\right)v_{\theta'}\right. \\ &\quad\left. + \int_0^{2\pi}\mathrm{d}\phi'\cos\phi'\int_0^{\pi}\mathrm{d}\theta'\sin\theta'\cos\theta'\eta\left(\mathbf{r}_\mathrm{p}^{'}\right)v_{\phi'}\right) =: 3\frac{\mathscr{L}}{\beta}(J_1 + J_2). \end{aligned} \quad (65)$$

The integrals J_1 and J_2 are evaluated as follows. By introducing the notations

$$Z_\ell^m(\theta') = \frac{\mathrm{d}P_\ell^m(\cos\theta')}{\mathrm{d}\theta'} \quad (66)$$

and

$$\begin{aligned} z_{\ell,m} &= \int_0^{\pi}\mathrm{d}\theta'\sin\theta' Z_\ell^m(\theta'), \\ p_{\ell,m} &= \int_0^{\pi}\mathrm{d}\theta'\cos\theta' P_\ell^m(\cos\theta'), \end{aligned} \quad (67)$$

after observing that

$$\begin{aligned} z_{\ell,-m} &\overset{(53)}{=} (-1)^m\frac{(\ell-m)!}{(\ell+m)!}z_{\ell,m}, \\ p_{\ell,-m} &\overset{(53)}{=} (-1)^m\frac{(\ell-m)!}{(\ell+m)!}p_{\ell,m}, \end{aligned} \quad (68)$$

and with

$$z_{\ell,m} \overset{(66)}{\underset{(67)}{=}} \left(\sin\theta' P_\ell^m(\cos\theta')\right)\Big|_0^{\pi} - \int_0^{\pi}\mathrm{d}\theta'\frac{\mathrm{d}\sin\theta'}{\mathrm{d}\theta'}P_\ell^m(\cos\theta') = -p_{\ell,m} \quad (69)$$

one arrives at

$$\begin{aligned} J_1 &:= \int_0^{2\pi}\mathrm{d}\phi'\sin\phi'\int_0^{\pi}\mathrm{d}\theta'\sin\theta'\left(-\frac{\beta R}{\mathscr{L}}\eta\left(\mathbf{r}_\mathrm{p}^{'}\right)v_{\theta'}\right) \\ &\overset{(59)}{\underset{(66)}{=}} \sum_{\ell=0}^{\infty}\sum_{m=-\ell}^{m=\ell}A_{\ell,m}\alpha_{\ell,m}\int_0^{\pi}\mathrm{d}\theta'\sin\theta' Z_\ell^m(\theta')\int_0^{2\pi}\mathrm{d}\phi'\sin\phi'\mathrm{e}^{im\phi'} \\ &= -i\pi\sum_{\ell=0}^{\infty}\sum_{m=-\ell}^{m=\ell}A_{\ell,m}\alpha_{\ell,m}z_{\ell,m}\left(\delta_{m,-1} - \delta_{m,1}\right) \\ &\overset{(68)}{\underset{(55)}{=}} i\pi\sum_{\ell=1}^{\infty}\left(A_{\ell,-1} + A_{\ell,1}\right)\alpha_{\ell,1}z_{\ell,1} \end{aligned}$$

(note that $z_{0,1} = 0$ due to $|m| \le \ell$) and

$$\begin{aligned} J_2 &:= \int_0^{2\pi}\mathrm{d}\phi'\cos\phi'\int_0^{\pi}\mathrm{d}\theta'\sin\theta'\cos\theta'\left(-\frac{\beta R}{\mathscr{L}}\eta\left(\mathbf{r}_\mathrm{p}^{'}\right)v_{\phi'}\right) \\ &\overset{(57)}{\underset{(60)}{=}} \sum_{\ell=0}^{\infty}\sum_{m=-\ell}^{m=\ell}imA_{\ell,m}\alpha_{\ell,m}\int_0^{\pi}\mathrm{d}\theta'\cos\theta' P_\ell^m(\cos\theta')\int_0^{2\pi}\mathrm{d}\phi'\cos\phi'\mathrm{e}^{im\phi'} \\ &= i\pi\sum_{\ell=0}^{\infty}\sum_{m=-\ell}^{m=\ell}mA_{\ell,m}\alpha_{\ell,m}p_{\ell,m}\left(\delta_{m,-1} + \delta_{m,1}\right) \\ &\overset{(68)}{\underset{(55)}{=}} i\pi\sum_{\ell=1}^{\infty}\left(A_{\ell,-1} + A_{\ell,1}\right)\alpha_{\ell,1}p_{\ell,1} \\ &\overset{(69)}{=} -i\pi\sum_{\ell=1}^{\infty}\left(A_{\ell,-1} + A_{\ell,1}\right)\alpha_{\ell,1}z_{\ell,1} = -J_1. \end{aligned}$$

Therefore $C_2 = 3\frac{\mathscr{L}}{\beta}(J_1 + J_2) = 0$, which verifies eqn (22).

Acknowledgements

P. M. thanks Dr Antonio Stocco for useful discussions and for providing the preprint version of ref. 22.

References

1 S. J. Ebbens and J. R. Howse, *Soft Matter*, 2010, **6**, 726–738.
2 E. Lauga and T. Powers, *Rep. Prog. Phys.*, 2009, **72**, 096601.
3 Y. Hong, D. Velegol, N. Chaturvedi and A. Sen, *Phys. Chem. Chem. Phys.*, 2010, **12**, 1423.
4 S. Sánchez, L. Soler and J. Katuri, *Angew. Chem., Int. Ed.*, 2015, **54**, 1414.
5 W. C. K. Poon, *Proceedings of the International School of Physics "Enrico Fermi", Course CLXXXIV "Physics of Complex Colloids"*, Amsterdam, 2013, p. 317.
6 J. El-Ali, P. K. Sorger and K. F. Jensen, *Nature*, 2006, **442**, 403.
7 A. Z. Wang, R. Langer and O. C. Farokhzad, *Annu. Rev. Med.*, 2012, **63**, 185–198.
8 J. L. Anderson, *Annu. Rev. Fluid Mech.*, 1989, **21**, 61.
9 R. Golestanian, T. B. Liverpool and A. Ajdari, *Phys. Rev. Lett.*, 2005, **94**, 220801.
10 S. Ebbens, M.-H. Tu, J. R. Howse and R. Golestanian, *Phys. Rev. E: Stat., Nonlinear, Soft Matter Phys.*, 2012, **85**, 020401.
11 T.-C. Lee, M. Alarcón-Correa, C. Miksch, K. Hahn, J. G. Gibbs and P. Fischer, *Nano Lett.*, 2014, **14**, 2407.
12 F. Jülicher and J. Prost, *Eur. Phys. J. E: Soft Matter Biol. Phys.*, 2009, **29**, 27.
13 M. Popescu, S. Dietrich and G. Oshanin, *J. Chem. Phys.*, 2009, **130**, 194702.
14 R. Kapral, *J. Chem. Phys.*, 2013, **138**, 202901.
15 B. ten Hagen, S. van Teeffelen and H. Löwen, *J. Phys.: Condens. Matter*, 2011, **23**, 194119.
16 R. Aveyard, *Soft Matter*, 2012, **23**, 8.
17 B. J. Park and D. Lee, *ACS Nano*, 2012, **6**, 782.
18 H. Rezvantalab and S. Shojaei-Zadeh, *Soft Matter*, 2013, **9**, 3640.
19 J. Bleibel, A. Domínguez, F. Günther, J. Harting and M. Oettel, *Soft Matter*, 2014, **10**, 2945.
20 J. Bleibel, A. Domínguez, M. Oettel and S. Dietrich, *Eur. Phys. J. E: Soft Matter Biol. Phys.*, 2011, **34**, 125.
21 M. Oettel, A. Domínguez and S. Dietrich, *Phys. Rev. E: Stat., Nonlinear, Soft Matter Phys.*, 2005, **71**, 051401.
22 X. Wang, M. In, C. Blanc, M. Nobili and A. Stocco, *Soft Matter*, 2015, **11**, 7376.
23 E. Lauga and A. M. J. Davis, *J. Fluid Mech.*, 2011, **705**, 120.
24 H. Masoud and H. A. Stone, *J. Fluid Mech.*, 2014, **741**, R4.
25 A. Würger, *J. Fluid Mech.*, 2014, **752**, 589.
26 A. Dominguez, P. Malgaretti, M. N. Popescu and S. Dietrich, *Phys. Rev. Lett.*, 2016, **116**, 078301.
27 J. Happel and H. Brenner, *Low Reynolds Number Hydrodynamics*, Prentice-Hall, Englewood Cliffs, NJ, 1965.
28 C. Pozrikidis, *J. Fluid Mech.*, 2007, **575**, 333.
29 C. Huh and L. Scriven, *J. Colloid Interface Sci.*, 1971, **35**, 85.
30 E. Dusan V. and S. Davis, *J. Fluid Mech.*, 1974, **65**, 71.
31 E. Dusan V., *J. Fluid Mech.*, 1976, **77**, 665.
32 L. Hocking, *J. Fluid Mech.*, 1976, **79**, 209.
33 M. E. O'Neill, K. B. Ranger and H. Brenner, *Phys. Fluids*, 1986, **29**, 913.
34 H. A. Stone and A. D. T. Samuel, *Phys. Rev. Lett.*, 1996, **77**, 4102.
35 H. A. Lorentz, *Zittingsversl. Koninkl. Akad. van Wetensch. Amsterdam*, 1896, **5**, 168.
36 H. K. Kuiken, *J. Eng. Math.*, 1996, **30**, 19.
37 P. Joseph and P. Taberling, *Phys. Rev. E: Stat., Nonlinear, Soft Matter Phys.*, 2005, **71**, 035303.
38 V. Sterr, R. Krauß, K. Morozov, I. Rehberg, A. Engel and R. Richter, *New J. Phys.*, 2009, **10**, 063029.
39 J. D. Jackson, *Classical Electrodynamics*, John Willey & Sons, New York, 1962.
40 J. R. Howse, R. A. L. Jones, A. J. Ryan, T. Gough, R. Vafabakhsh and R. Golestanian, *Phys. Rev. Lett.*, 2007, **99**, 048102.
41 H. Risken, *The Fokker-Planck Equation*, Springer-Verlag, Berlin, 1988.
42 A. Pototsky, U. Thiele and H. Stark, *Phys. Rev. E: Stat., Nonlinear, Soft Matter Phys.*, 2014, **90**, 030401.
43 G. Boniello, C. Blanc, D. Fedorenko, M. Medfai, N. Ben Mbarek, M. In, M. Gross, A. Stocco and M. Nobili, *Nat. Mater.*, 2015, **14**, 908.